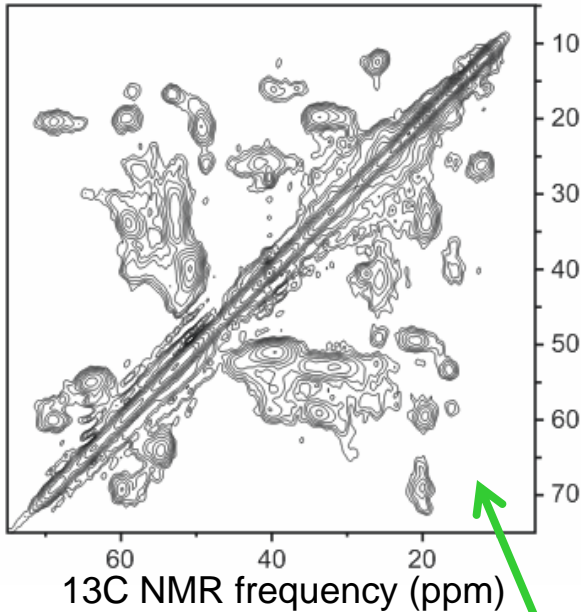


Advanced topics in solid state NMR, R. Tycko

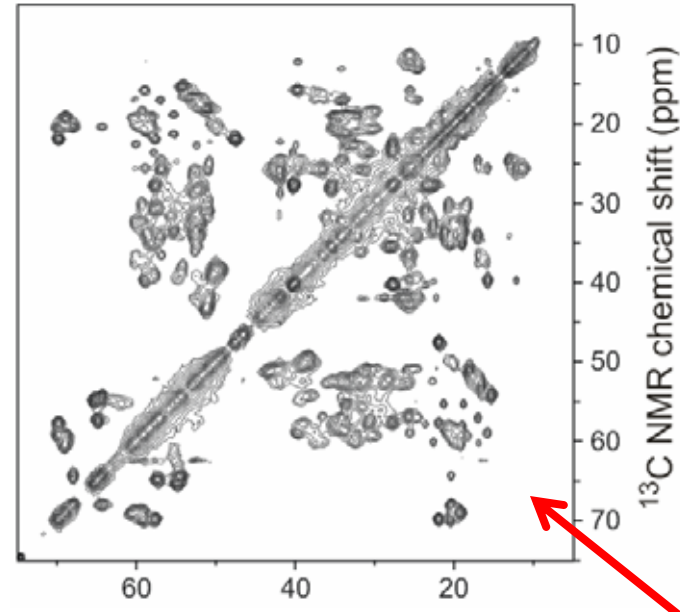
1. Isotopic labeling strategies and sample preparations for amyloid fibrils (and other systems?)
2. Low-temperature MAS
3. Quantitative distance measurements by homonuclear recoupling in uniformly or multiply labeled samples

1. Isotopic labeling strategies, etc.

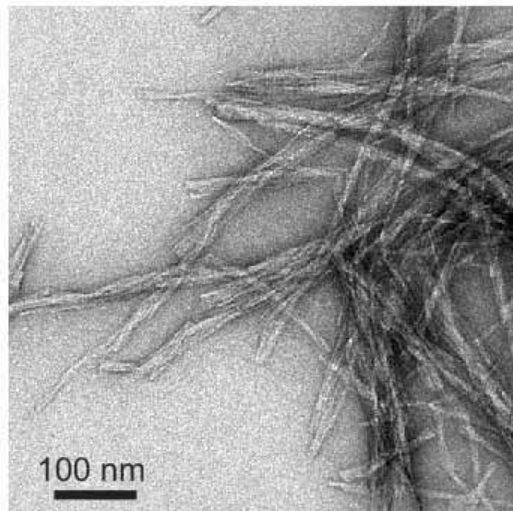
U-labeled Ure2p₁₋₈₉ fibrils



U-labeled HET-s₂₁₈₋₂₈₉ fibrils



Note: lyophilized,
then rehydrated
in the MAS rotor



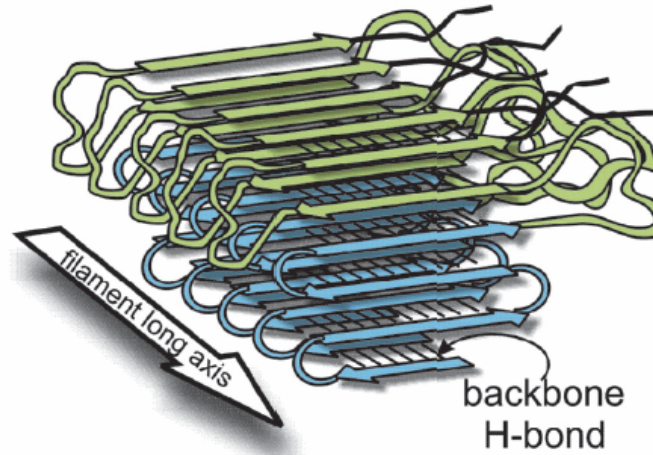
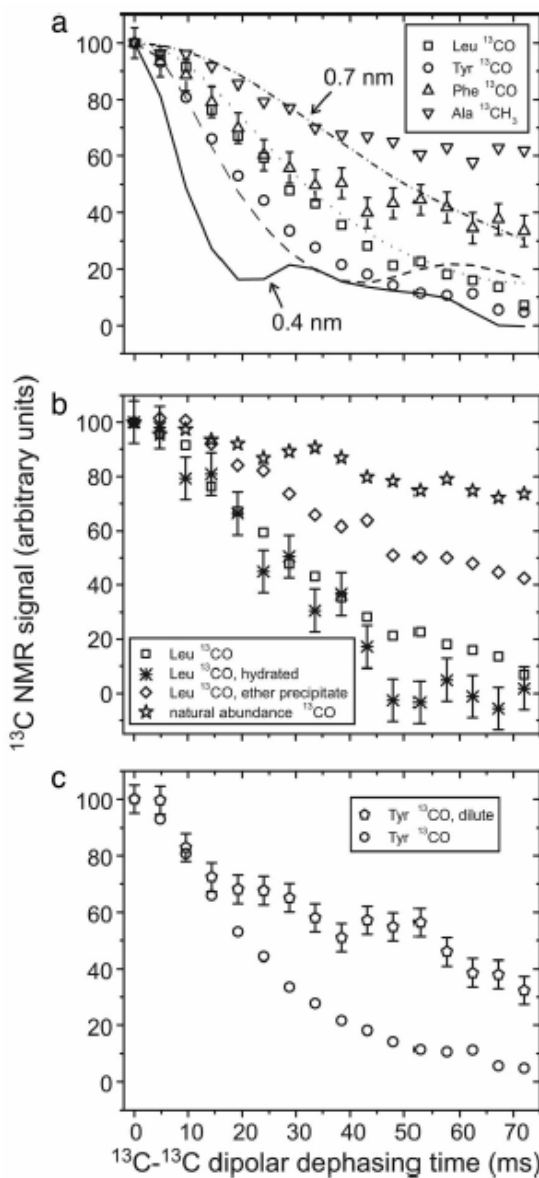
Can make great progress towards
full 3D structure determination
(B. Meier, R. Riek, et al.)

Can not determine full 3D structure, but
still can address real scientific questions.

Baxa et al., Biochemistry 2007

1. Isotopic labeling strategies, etc.

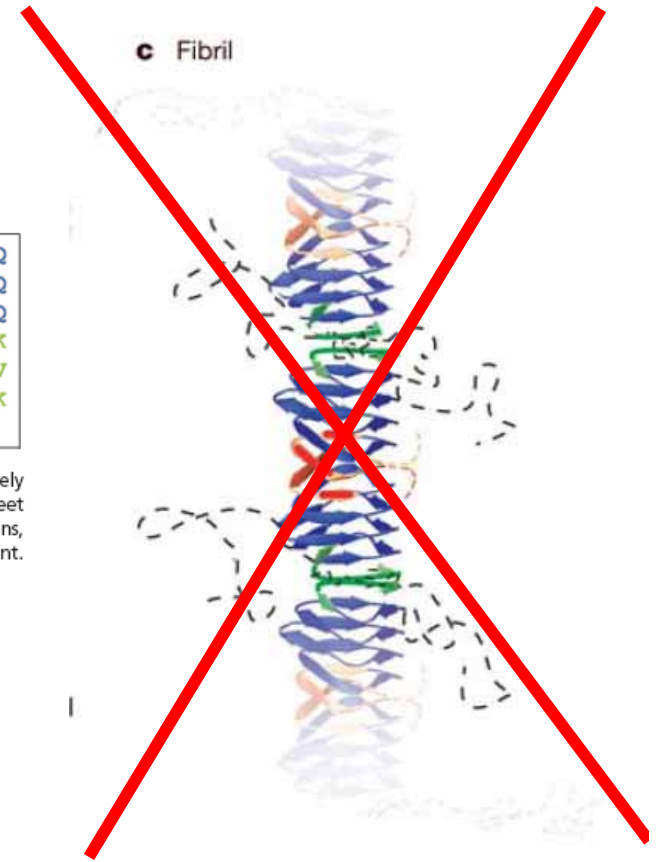
Sup35NM fibrils, selective labeling of amino acid types



MSDSNQGNNQ	QNYQQYSQNG	NQQQGNNRYQ	GYQAYNAQAQ
PAGGYQNYQ	GYSGYQQGGY	QQYNPDAGYQ	QQYNPQGGYQ
QYNPQGGYQQ	QFNPQGGRGN	YKNFNYNNNL	QGYQAGFQPQ
SQGMSLNDFQ	KQQKQAAPKP	KKTLKLVSSS	GIKLANATKK
VGTKPAESDK	KEEKSAETK	EPTKEPTKVE	EPVKKEEKPV
QTEKTEEKS	ELPKVEDLKI	SESTHTNNA	NVTSADALIK
EQEEVDDEV	VND		

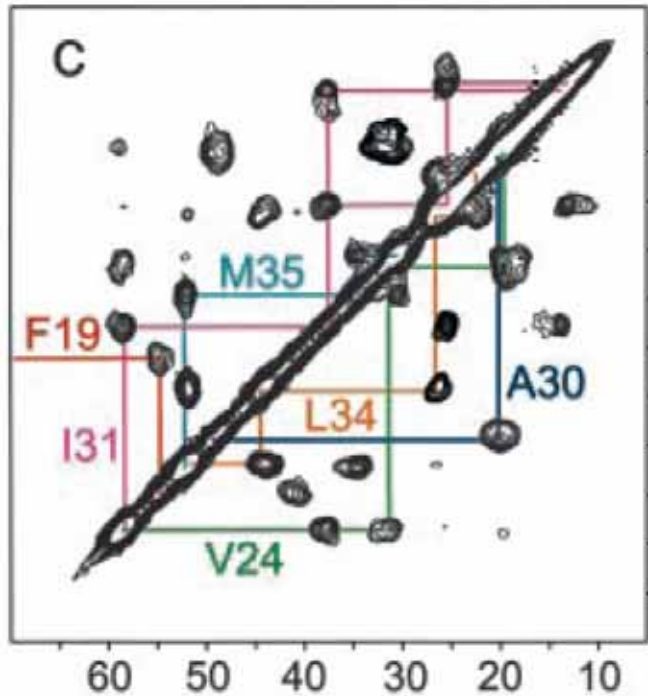
Fig. 4. Tentative model of Sup35NM amyloid. The N domain (blue) is largely β -sheet, whereas the M domain (green) consists of both β -sheet and non- β -sheet regions. The model is schematic and does not pretend to portray the locations, number, or lengths of β -strands or loops, which may depend on the prion variant.

Shewmaker et al., PNAS 2006



Krishnan and Lindquist, Nature 2005

1. Isotopic labeling strategies, etc.



$A\beta_{1-40}$ fibrils, U-labeled at specific sites by solid-phase synthesis. Dry lyophilized, somewhat polymorphic (Petkova et al., PNAS 2002) linewidths $\sim 2.0-2.5$ ppm

Petkova et al., Science 2005

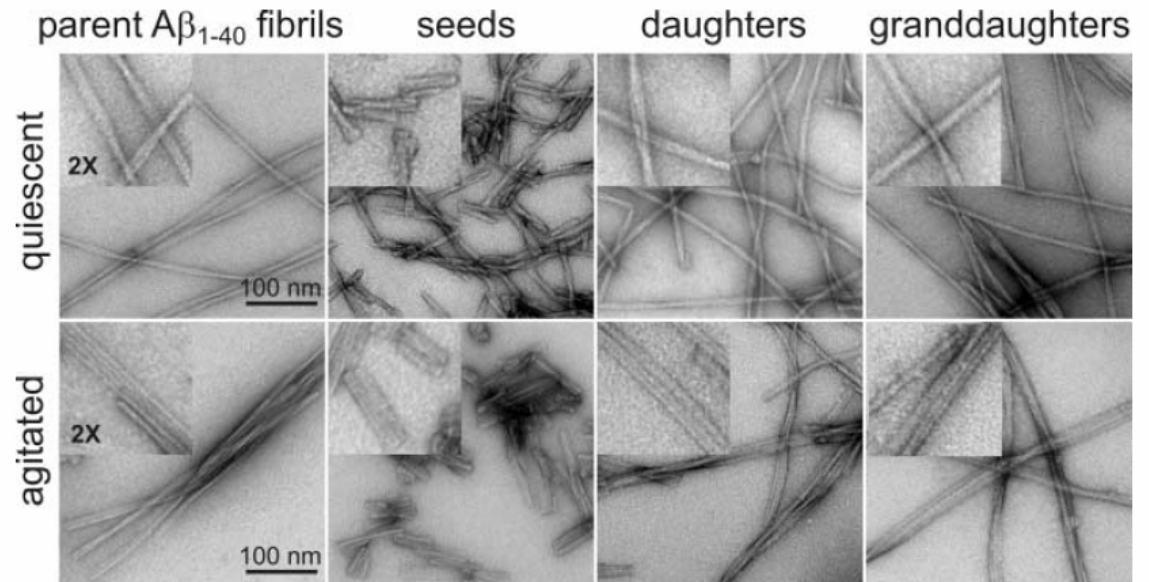
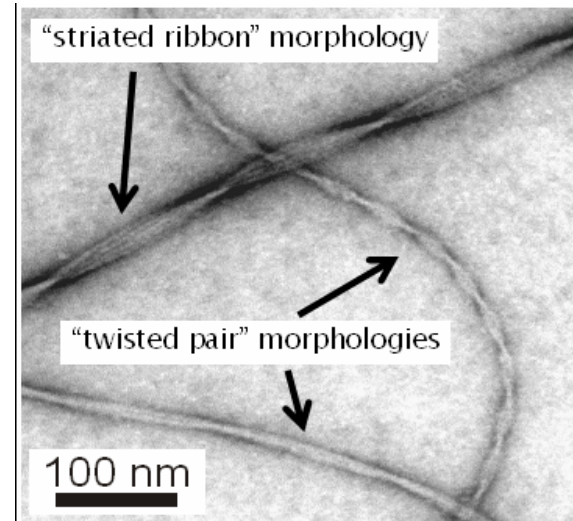


Fig. 1. TEM images of amyloid fibrils formed by the $A\beta_{1-40}$ peptide, negatively stained with uranyl acetate. Parent fibrils were prepared by incubation of $A\beta_{1-40}$ solutions either under quiescent dialysis conditions or in a closed polypropylene tube with gentle agitation. Daughter and granddaughter fibrils were grown under dialysis from solutions that were seeded with sonicated fragments of parent and daughter fibrils, respectively.

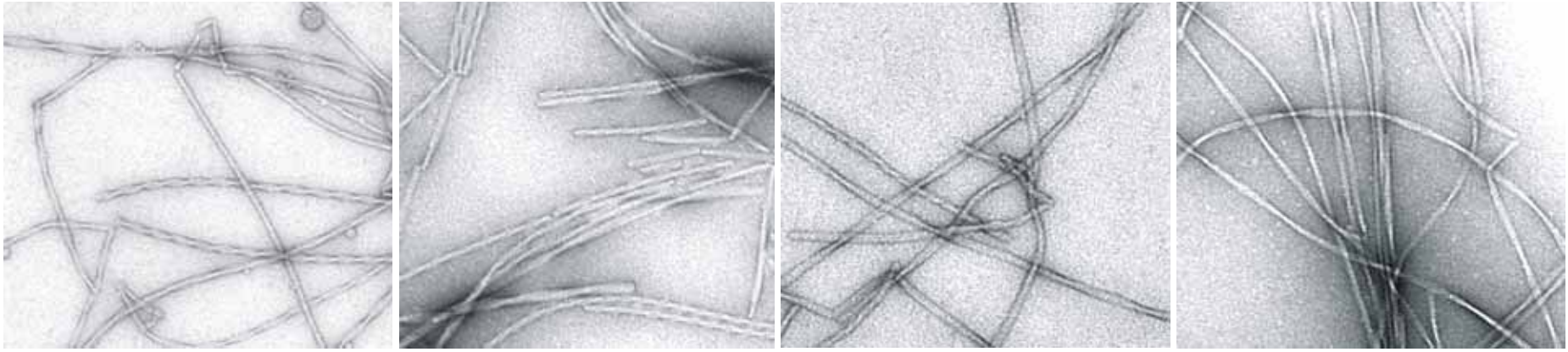
Self-purification by multiple rounds of sonication/seeding/growth (Anant Paravastu)

1

2

5

12 rounds

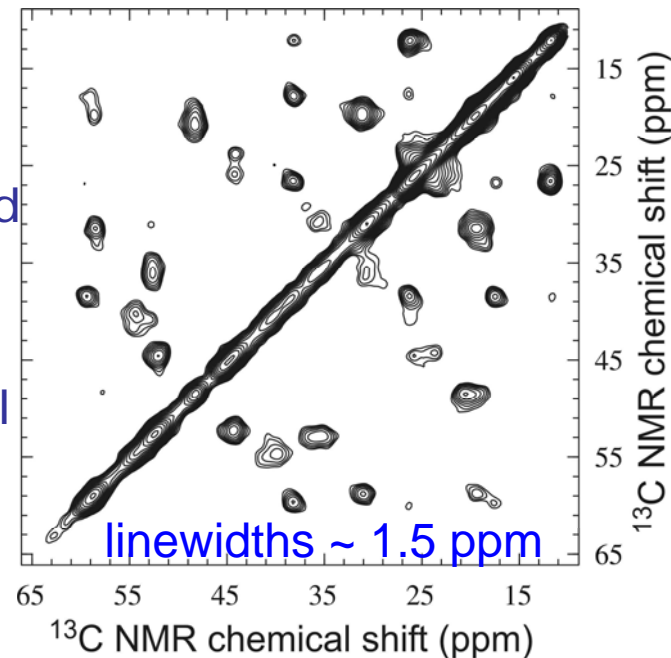


Solid state NMR, U-labeled F19,
V24, G25, A30, I31, L34, M35

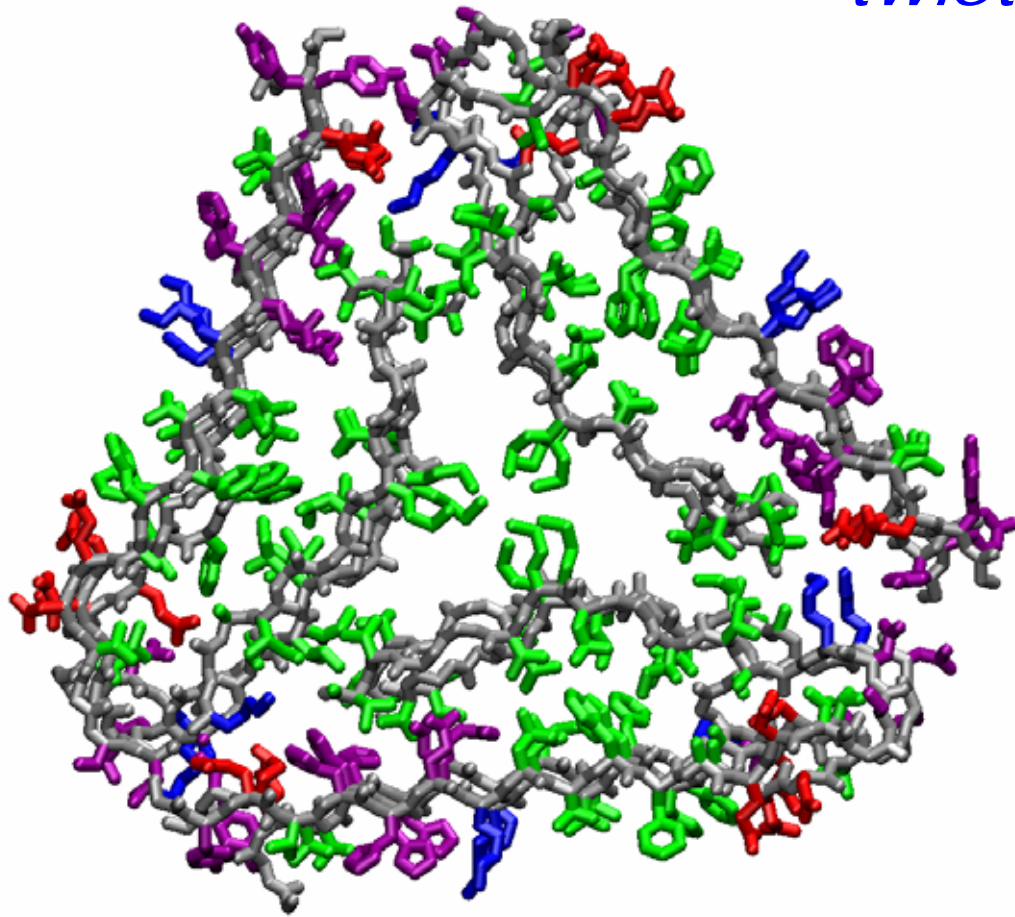
Single, sharp line for each ^{13}C -labeled
site.





All molecules have the same
conformation and the same structural
environment.

IMPLIES 3-FOLD SYMMETRY.

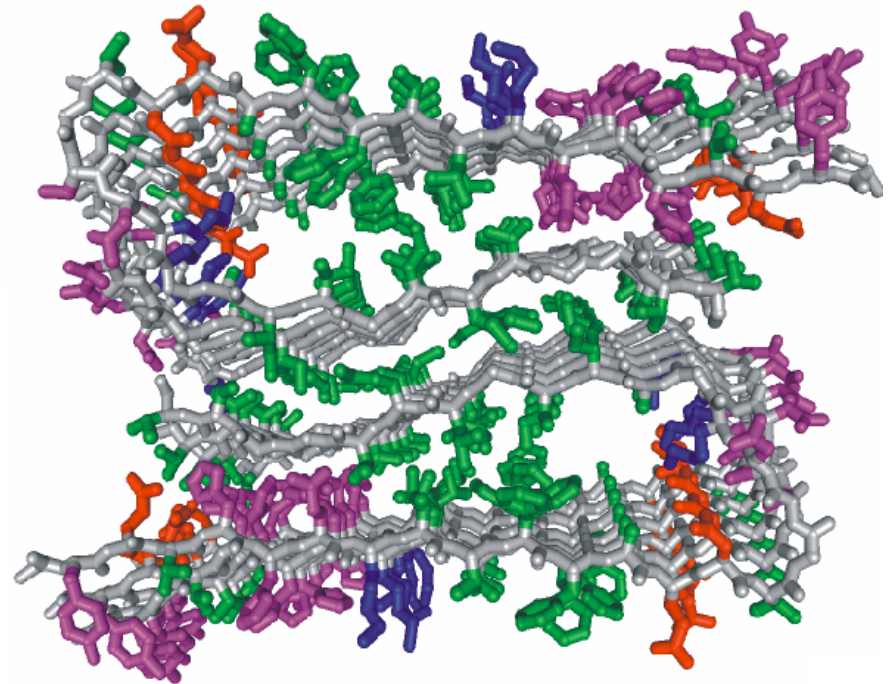


"twisted pair" $A\beta_{1-40}$ fibril structure

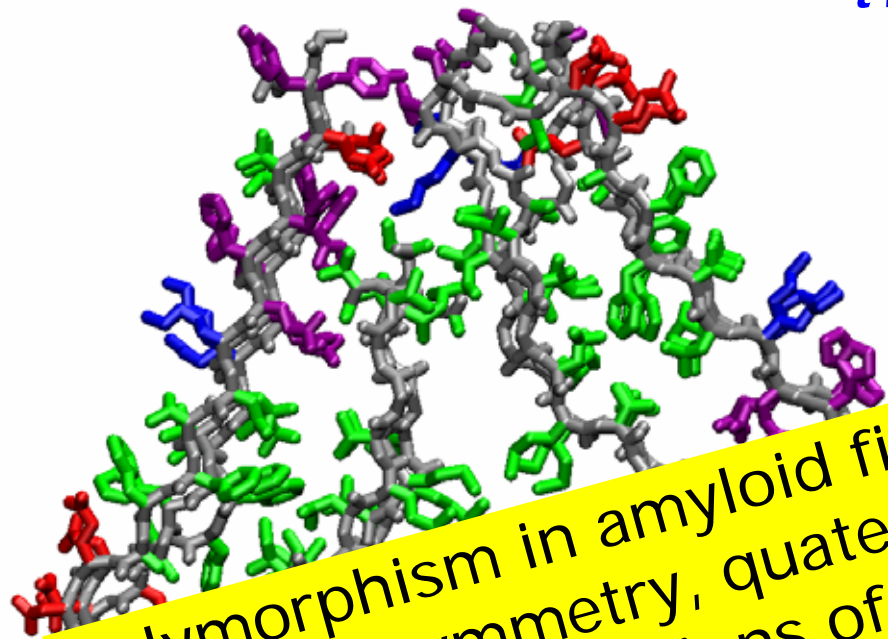


-  hydrophobic
-  negatively charged
-  positively charged
-  polar

"striated ribbon" $A\beta_{1-40}$ fibril structure

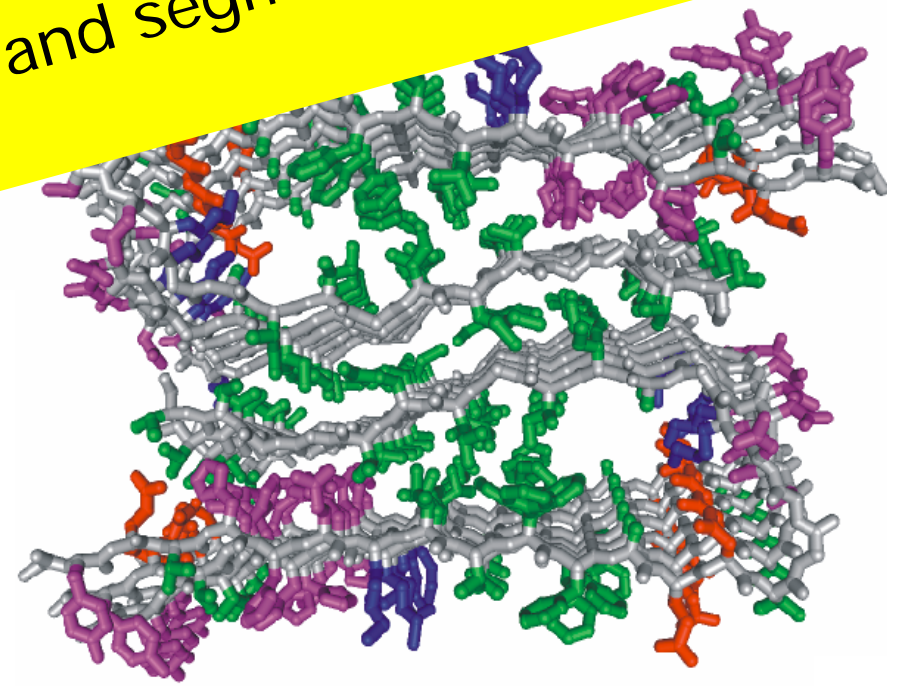


"twisted pair" $A\beta_{1-40}$ fibril structure



Polymorphism in amyloid fibrils arises from variations in overall symmetry, quaternary structure and the detailed conformations of non- β -strand segments. (but not the location of β -strand segments or the type of β -sheets)

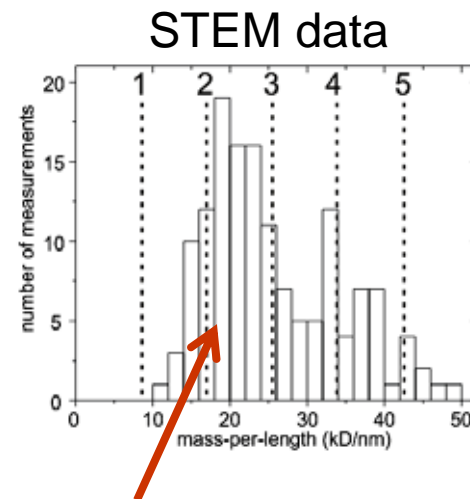
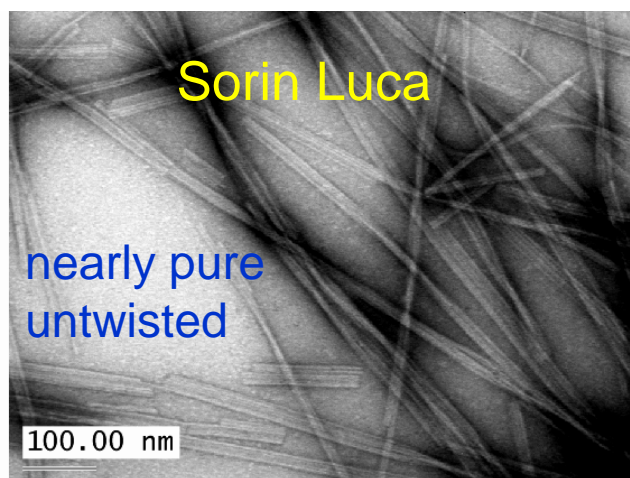
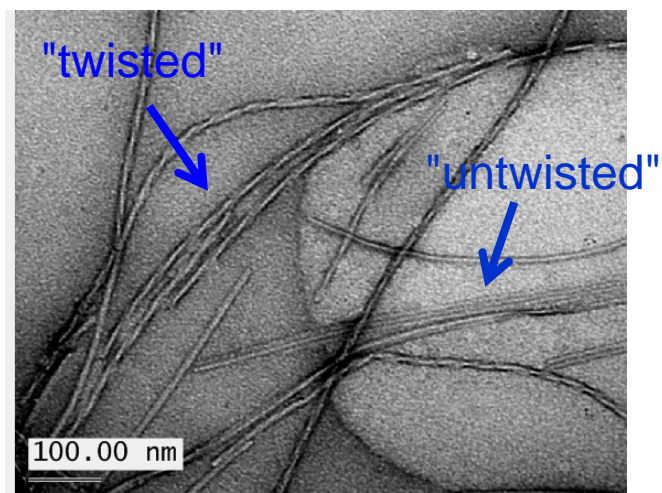
"striated ribbon" $A\beta_{1-40}$ fibril structure



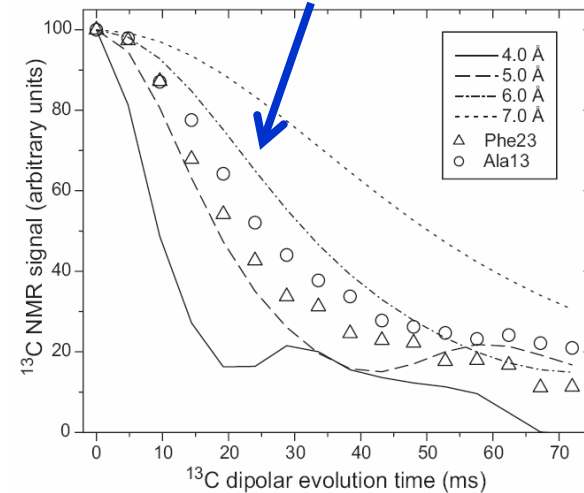
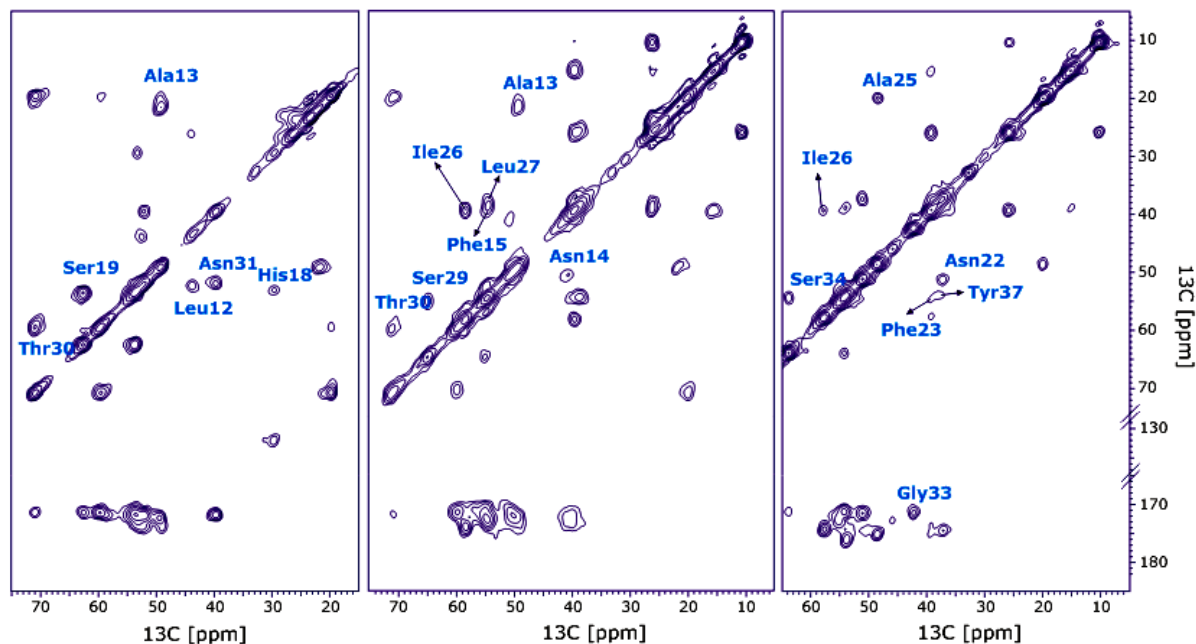
Universality of amyloid structure

amylin (a.k.a. islet amyloid polypeptide, IAPP):

KCNTATCAT**Q**RLAN**FLVHSSNNFGAILSSTNVGSNTY**



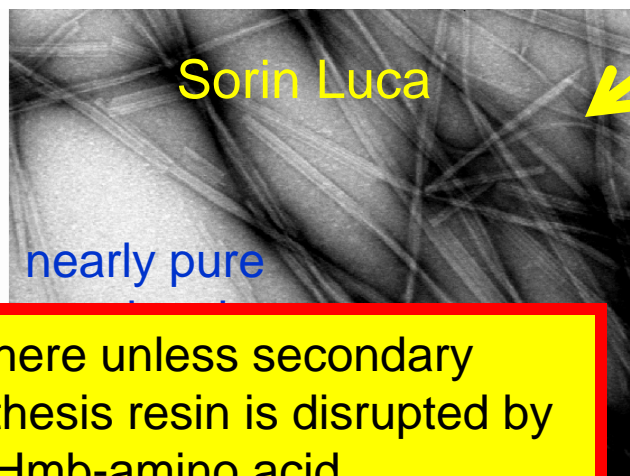
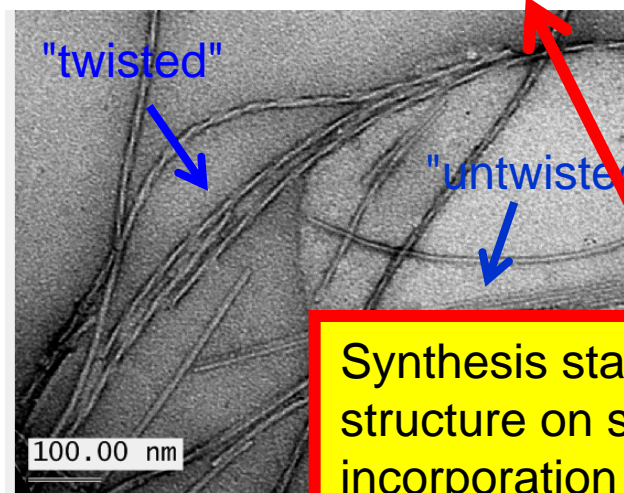
amylin protofilament contains two cross- β units parallel β -sheets



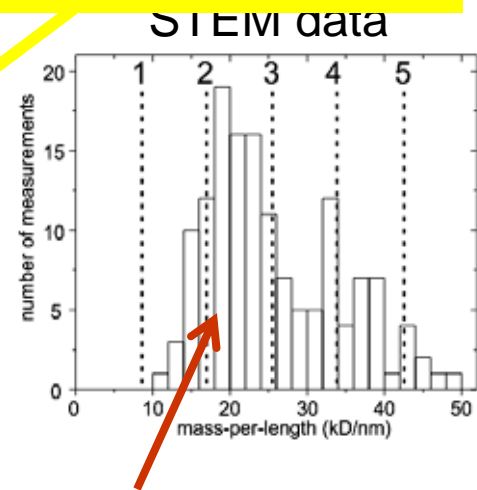
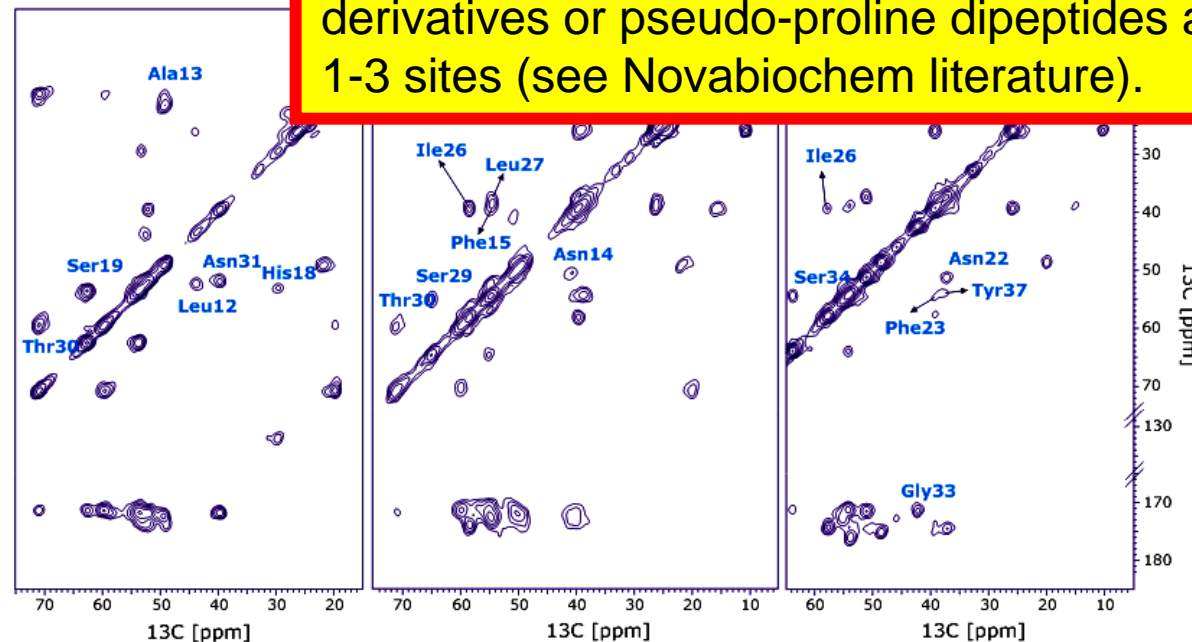
Universality of amyloid structure

amylin (a.k.a. islet amyloid polypeptide, I
KN**T**A**T**CA**T**Q**R**L**A****N****F****L****V****H****S****S****N****N****F****G****A****I****L****S****S****T**

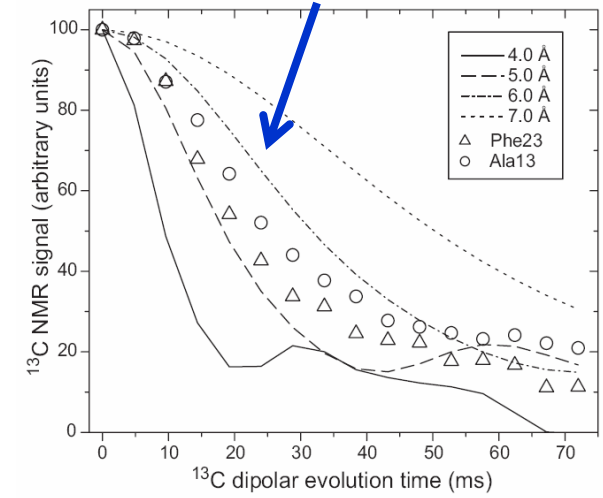
purification of monomers by gel filtration, seeded growth



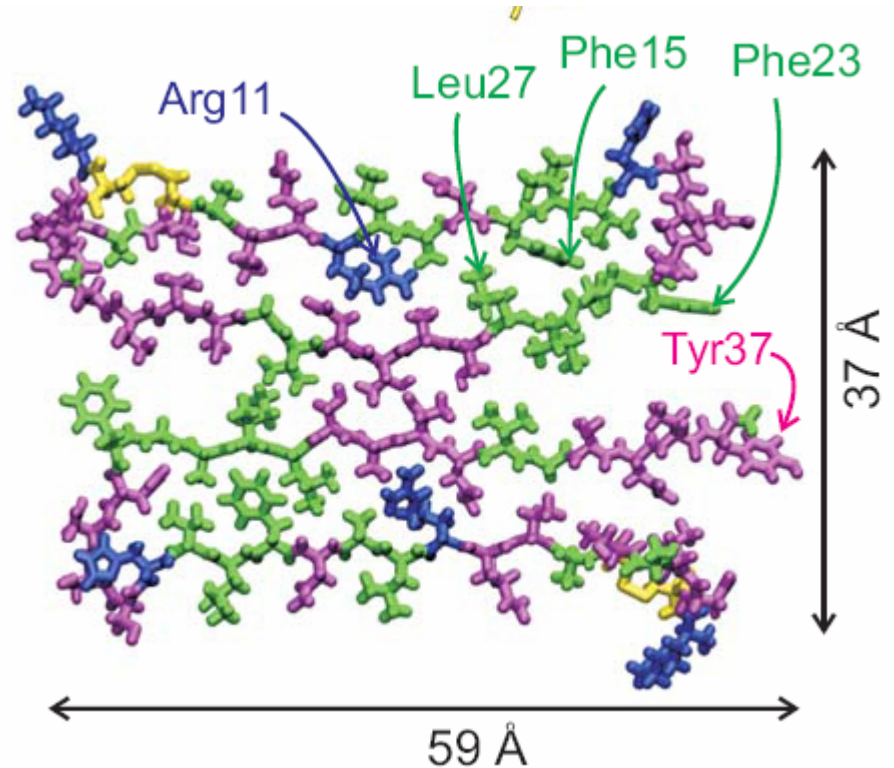
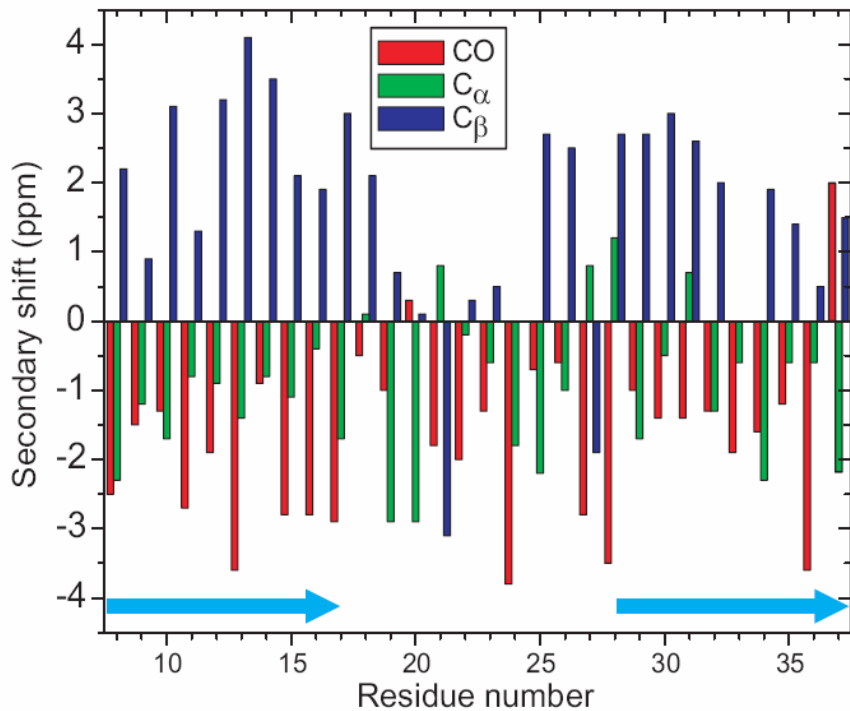
Synthesis stalls here unless secondary structure on synthesis resin is disrupted by incorporation of Hmb-amino acid derivatives or pseudo-proline dipeptides at 1-3 sites (see Novabiochem literature).



amylin protofilament contains two cross- β units parallel β -sheets



amylin (a.k.a. islet amyloid polypeptide, IAPP):
KCNTATCAT**Q**RLAN**F**LVHSSNN**F**GAILSS**T**NVGSNT**Y**

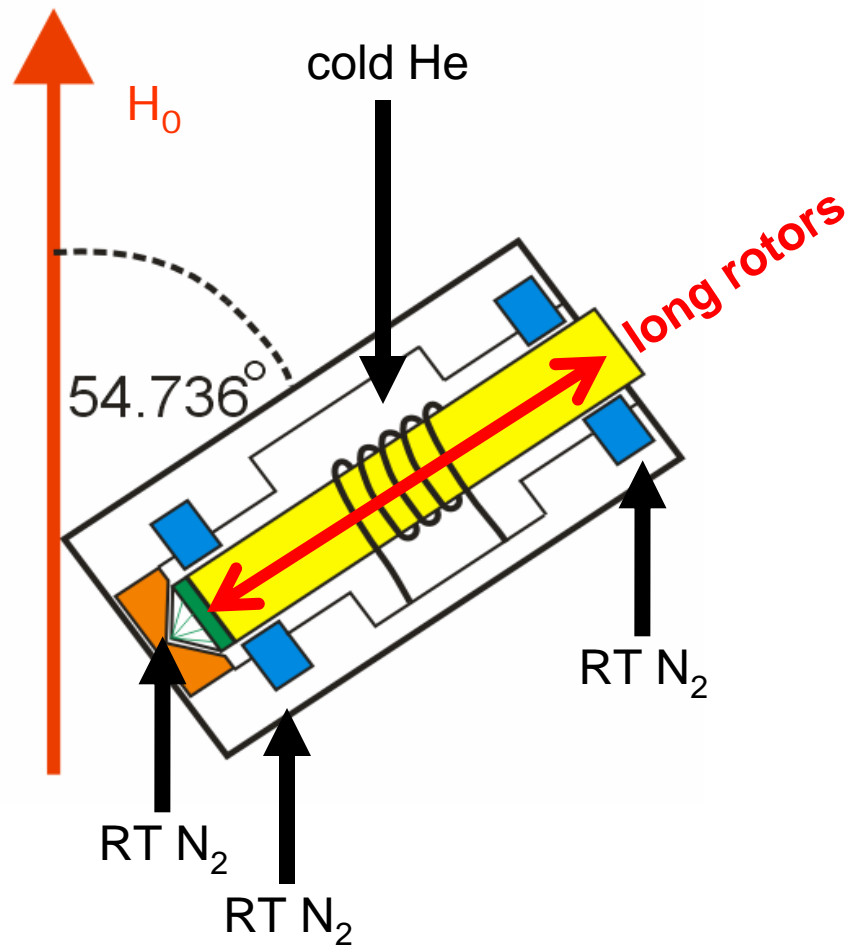


- disordered, disulfide-bridged N-terminal segment
- two β -strand segments, forming parallel β -sheets
- two-fold symmetry about fibril axis
- closely resembles A β_{1-40} fibril structure

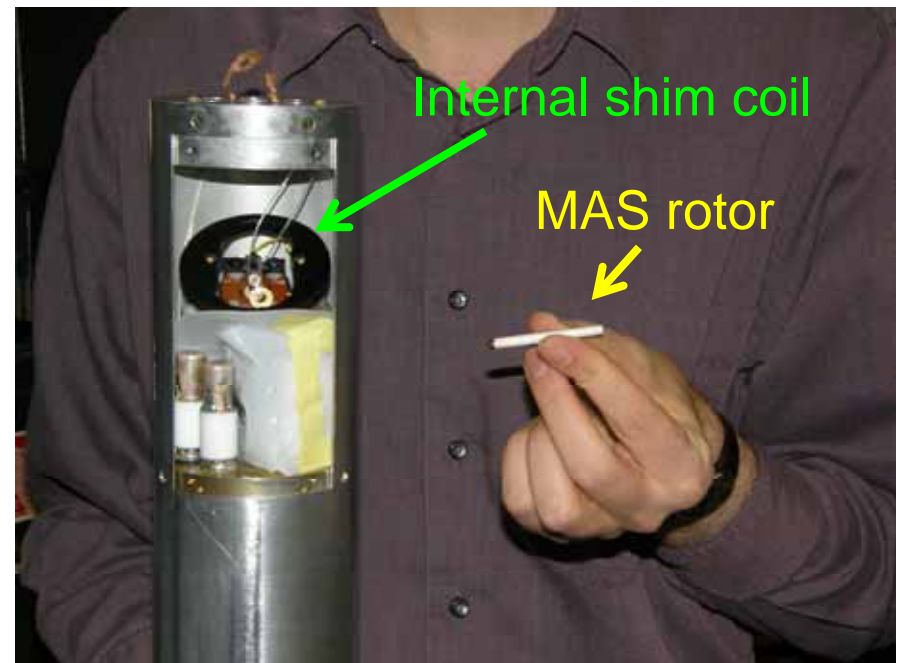
- hydrophobic
- negatively charged
- positively charged
- polar

Luca et al., Biochemistry 2007

2. Low-temperature MAS



experiment time $\sim 1/T^2 - 1/T^3$



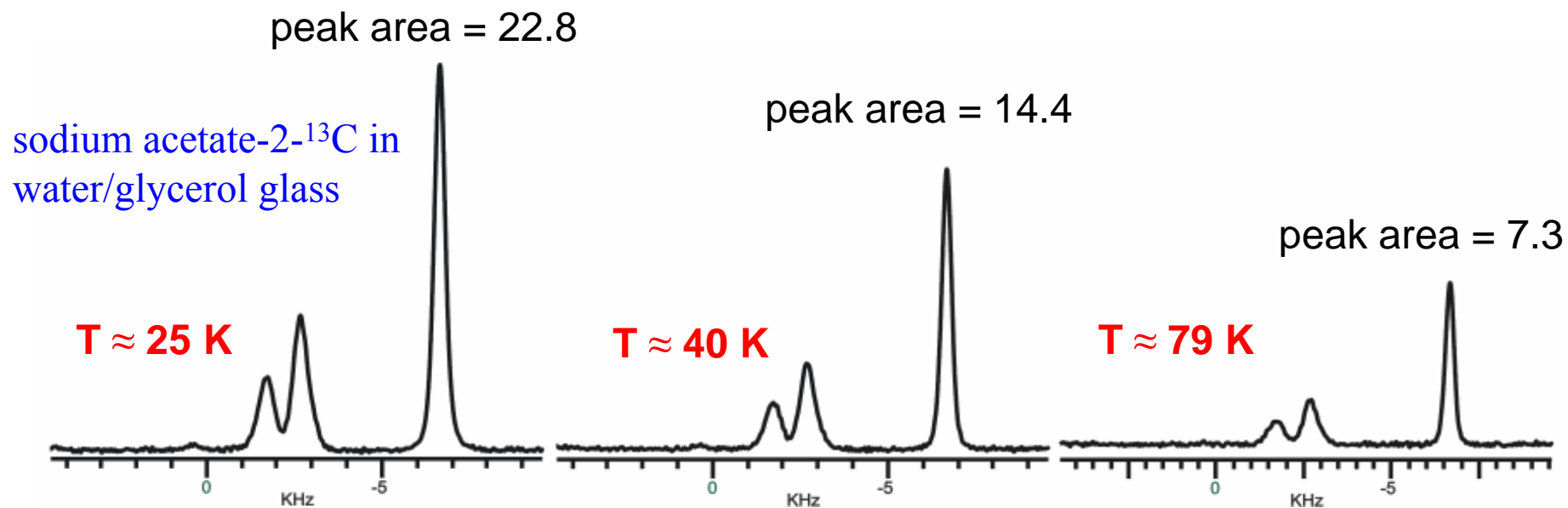
Current Probe Properties

**25 K sample temperature at 6.7 kHz spinning and 3 liters/hour liquid He
Sample volume 50ul, 1H decoupling 75 kHz, 100 kHz usable for a few ms.**

**4 mm outer diameter rotor, based on Varian spinner housing with longer rotor.
Liquid He cooling sample, room temperature nitrogen bearing and drive gas.
Teflon coated wire used for coil, Teflon enclosure around coil and sample region
insulates helium cooled region from nitrogen gas.**

Spinning stable (5 Hz) (runs have currently lasted up to ~10 hours.)

**Dysprosium EDTA used to provide fluctuating electron spin to have reasonable
1H relaxation rate at low temperatures.**



Magic-angle spinning at 7.00 kHz

Proton decoupling at 105 kHz

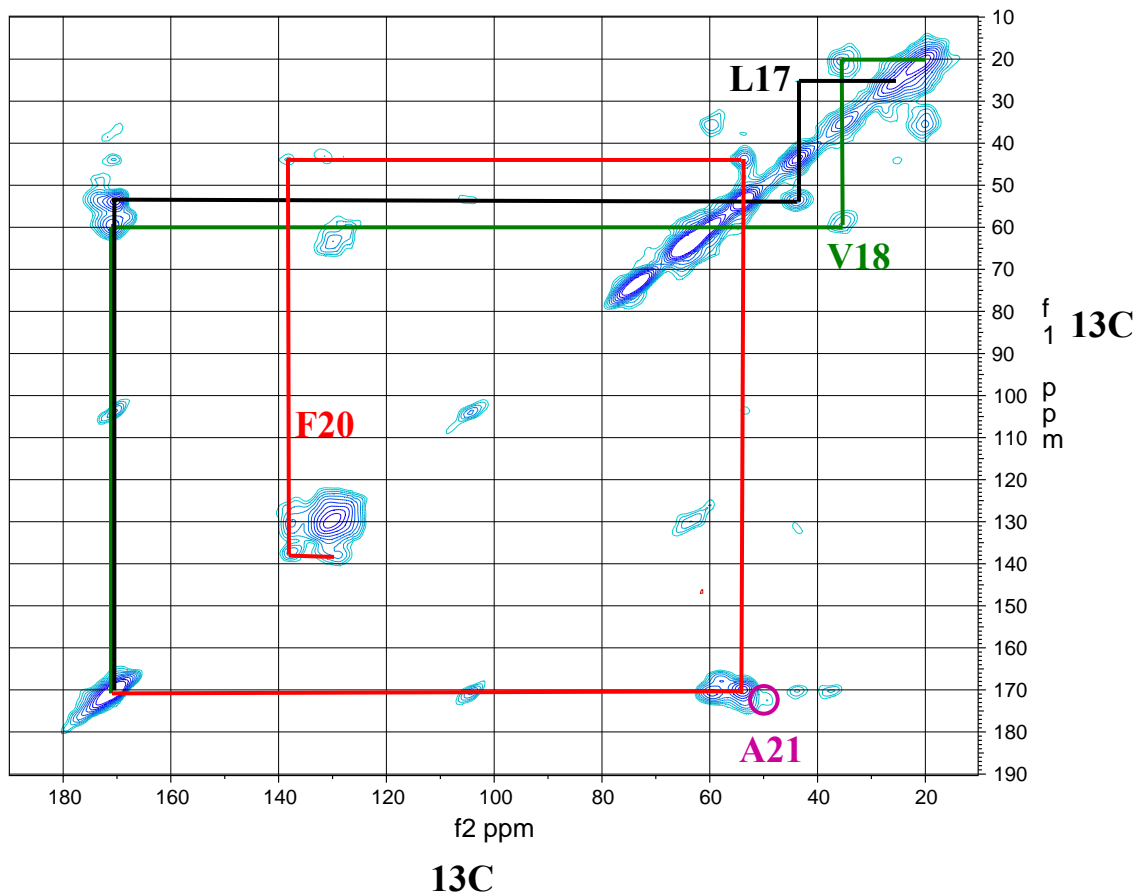
Proton $T_1 \approx 6$ s at 25 K, with 200 μ M Dy-EDTA

NMR linewidths < 1.4 ppm

Helium consumption \sim 2 liters per hour

Abeta 14-23 amyloid fibrils

2D ^{13}C - ^{13}C correlation by RFDR pulse sequence



25 K, 6.7 kHz spin, 2080 total scans for 2D,
1H T1 = 4 sec, repeat rate 6 sec,
time required = 3.5 hours

Abeta 14-23

amino acid sequence: **HQKLVF**FA**ED**

1.7 mg of sample labeled at V18, F20

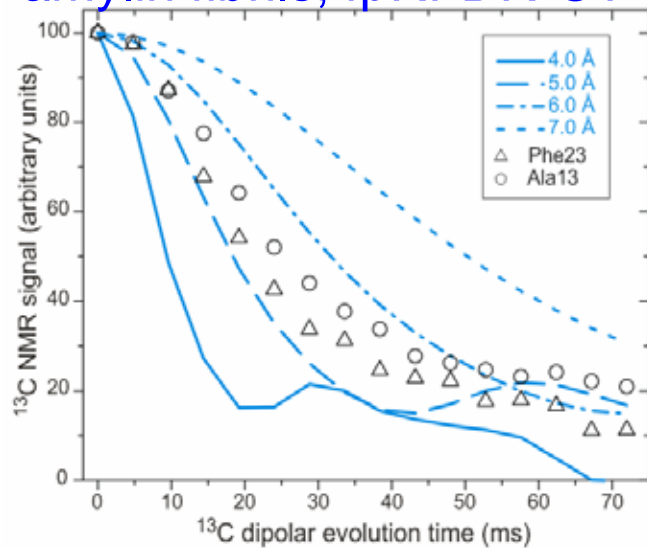
1.0 mg of sample labeled at L17, A21

hydrated with 10ul of 200uM DyEDTA in
25 mol% glycerol.

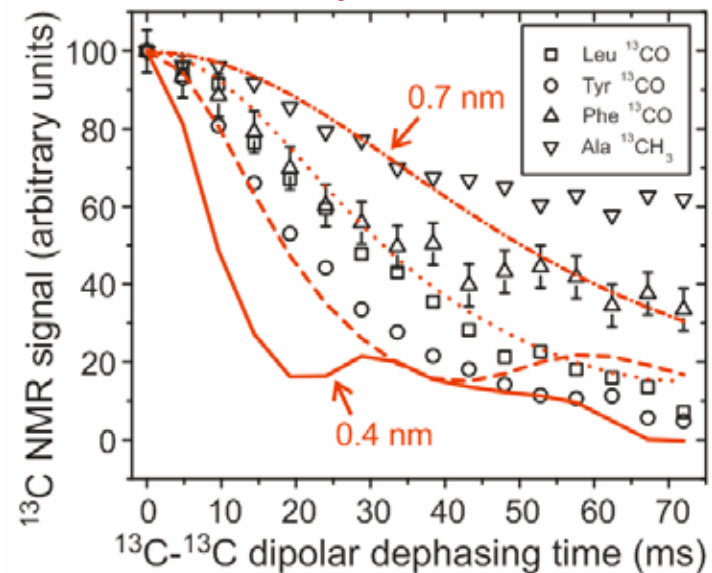
3. Quantitative distance measurements with homonuclear dipolar recoupling

works well for selectively labeled samples:

amylin fibrils, fpRFDR-CT data

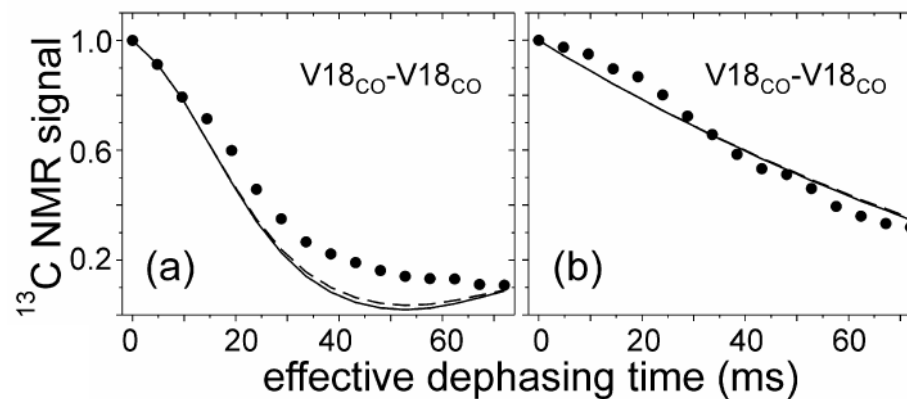


Sup35NM fibrils



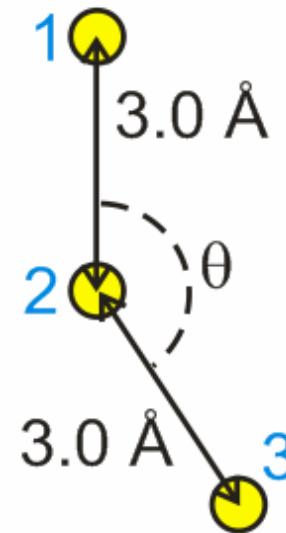
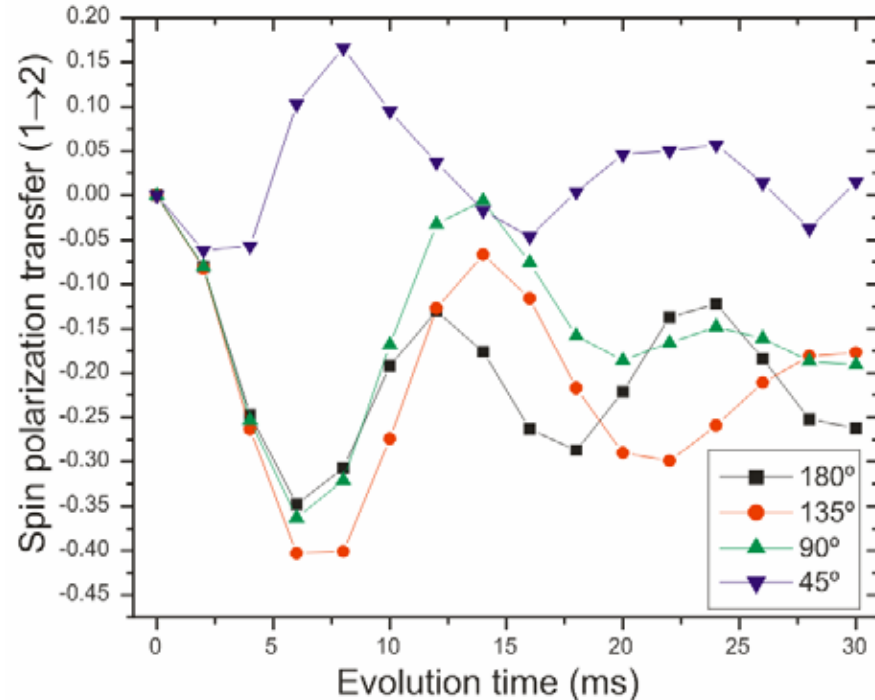
pH 7.4 fibrils

pH 2.4 fibrils



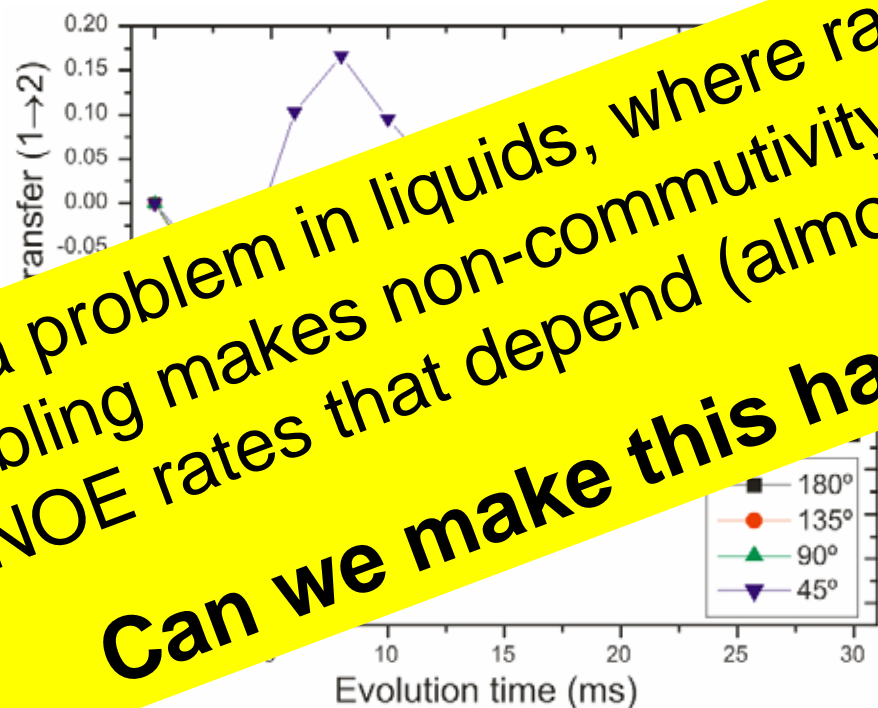
A β_{11-25} fibrils

In uniformly or multiply labeled solids, recoupling data depend on the full geometry, not only the pairwise internuclear distances. This is a consequence of the non-commutivity of pairwise dipole-dipole couplings.



simulations, POST-C7 recoupling, MAS at 8 kHz, ^{13}C NMR at 14.1 T, isotropic shifts = 20 ppm, -20 ppm, 5 ppm

In uniformly or multiply labeled solids, recoupling data depend on the full geometry, not only the pairwise internuclear distances. This is a consequence of the non-commutivity of pairwise dipole-dipole



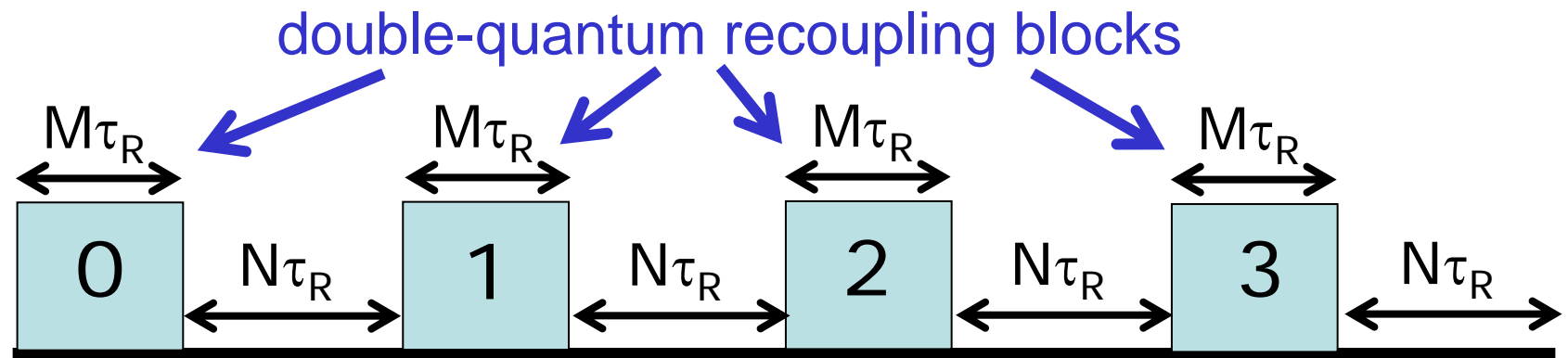
Not a problem in liquids, where random molecular tumbling makes non-commutivity unimportant, leading to NOE rates that depend (almost) purely on distances.

Can we make this happen in solids??

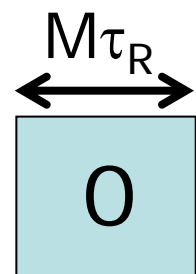


simulations, POST-C7 recoupling, MAS at 8 kHz, ^{13}C NMR at 14.1 T, isotropic shifts = 20 ppm, -20 ppm, 5 ppm

Stochastic homonuclear dipolar recoupling

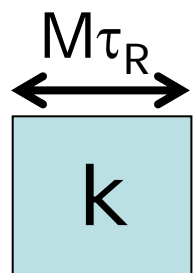


random carrier frequency offsets



$$H_{\text{eff}}^{(0)} = dI_+S_+ + d^*I_-S_-$$

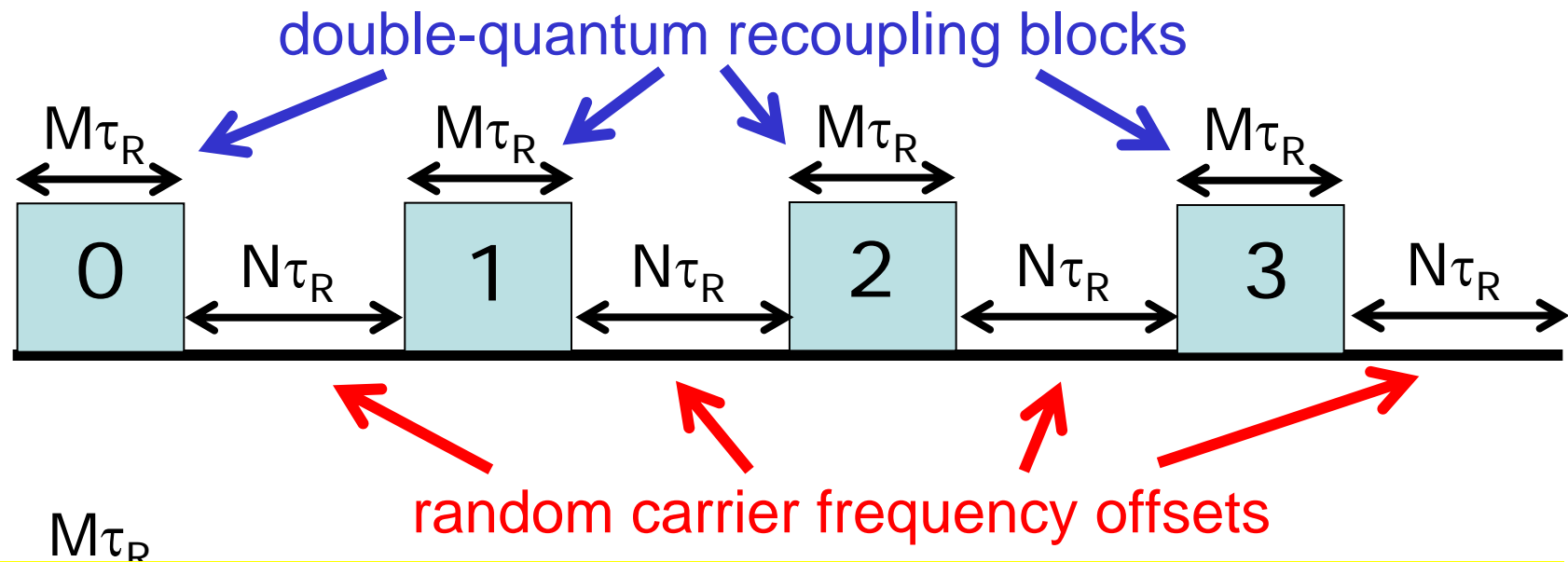
random phase modulation



$$H_{\text{eff}}^{(k)} = dI_+S_+e^{-i\phi_{IS}(k)} + d^*I_-S_-e^{i\phi_{IS}(k)}$$

$$\text{where } \phi_{IS}(k) = \sum_{j=1}^k N[\Delta\omega_I(j) + \Delta\omega_S(j)]\tau_R$$

Stochastic homonuclear dipolar recoupling



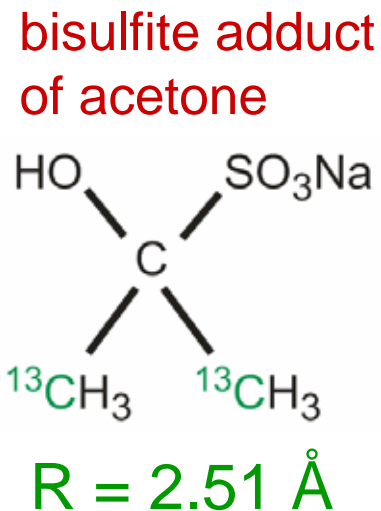
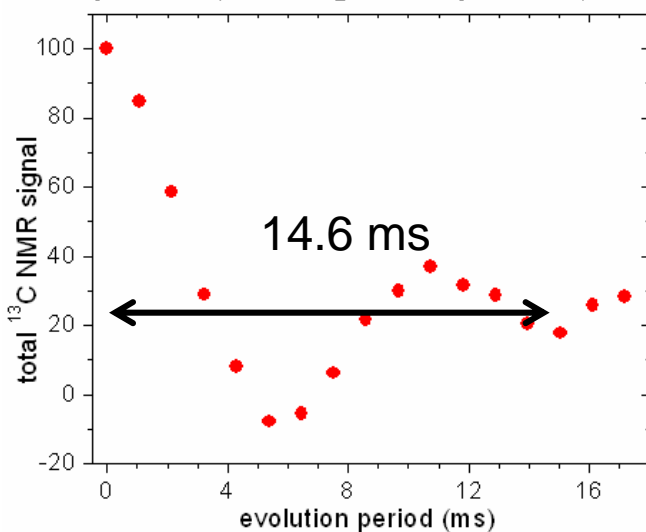
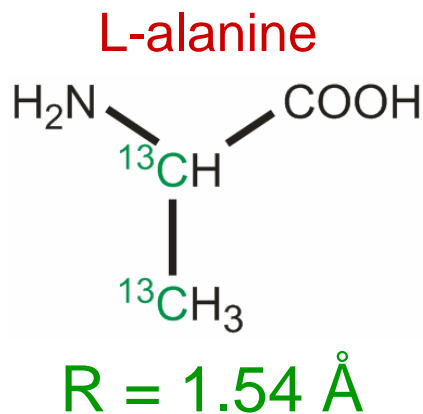
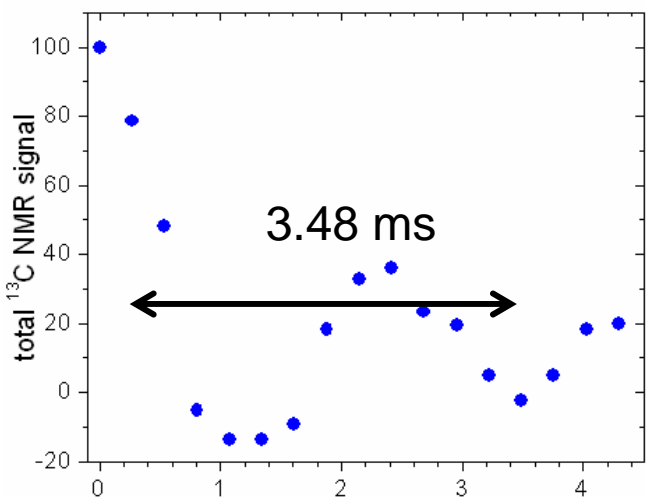
All pairwise couplings average to zero, but in a stochastic and (almost) uncorrelated way.

Coherent polarization transfers become incoherent, described by rates that are proportional to $1/R^6$ (NOE-like).

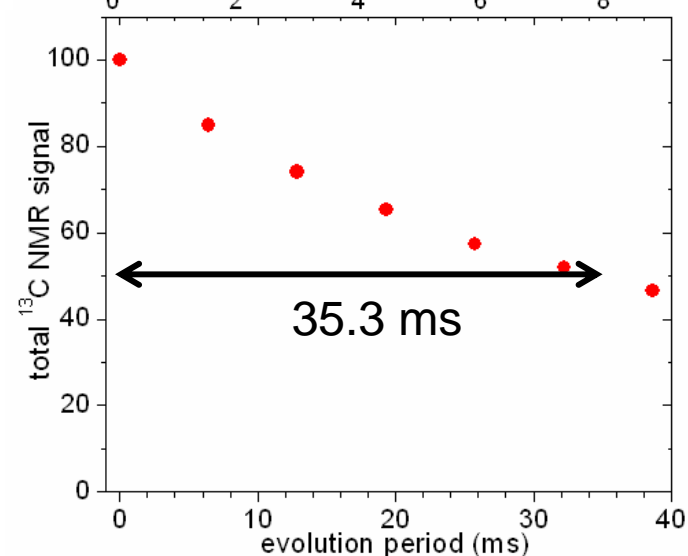
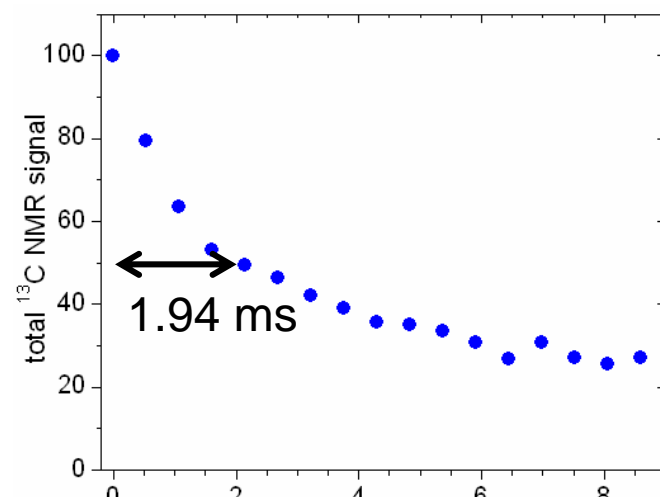
$$\text{where } \phi_{IS}(k) = \sum_{j=1}^N N[\Delta\omega_I(j) + \Delta\omega_S(j)]\tau_R$$

Experimental demonstrations of stochastic recoupling, two-spin systems

coherent



stochastic



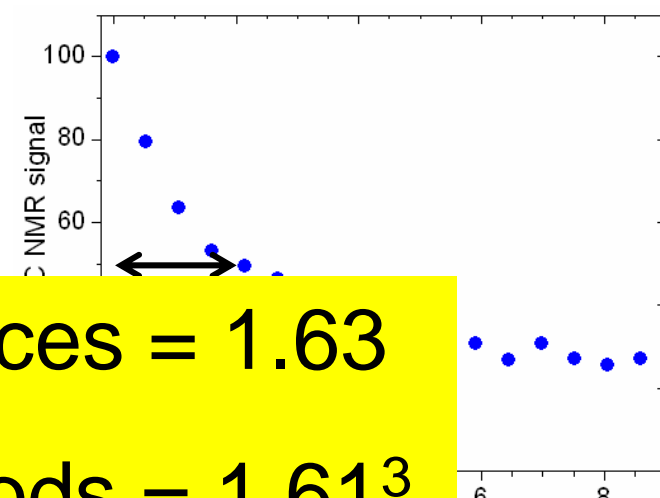
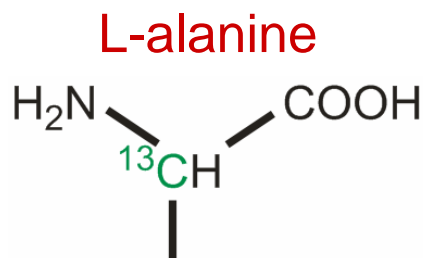
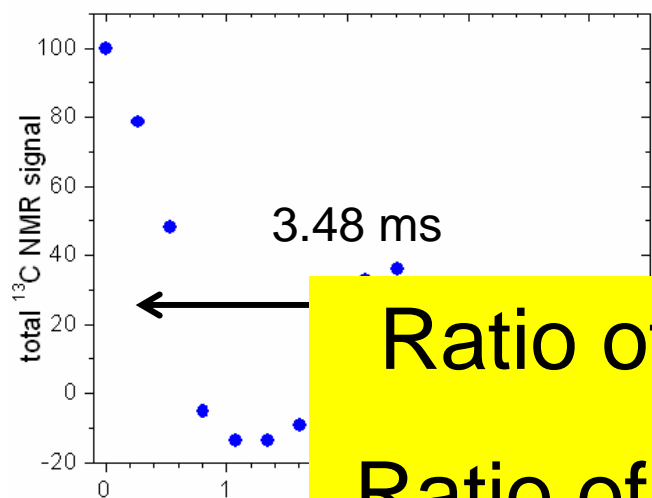
(POST-C7 recoupling, 7.45 kHz MAS, 9.4 T)

Experimental demonstrations of stochastic recoupling, two-spin systems

coherent

two-spin systems

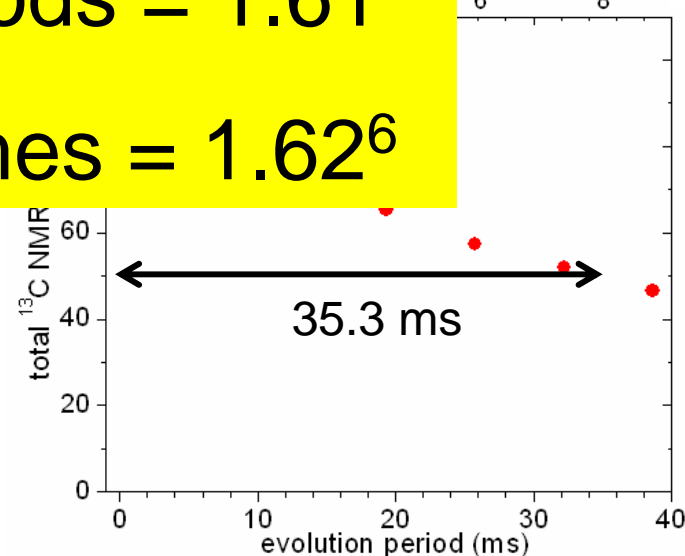
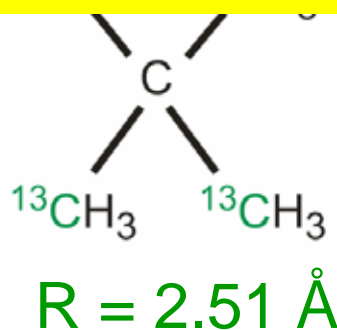
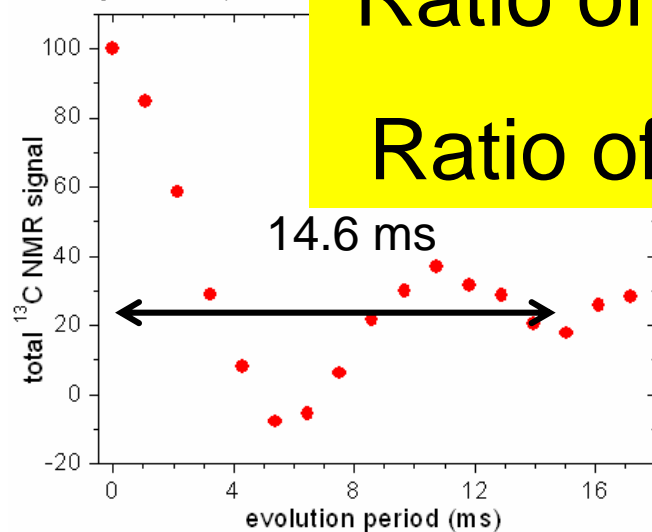
stochastic



Ratio of ^{13}C - ^{13}C distances = 1.63

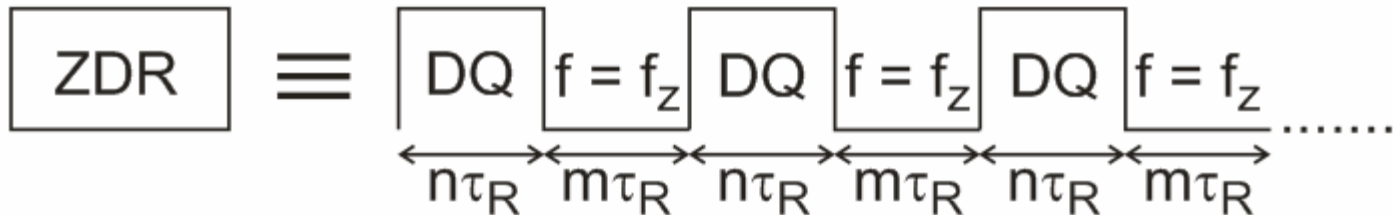
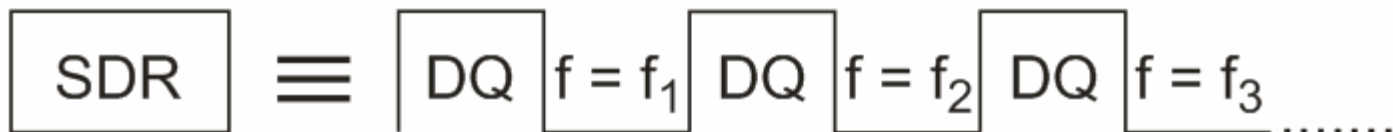
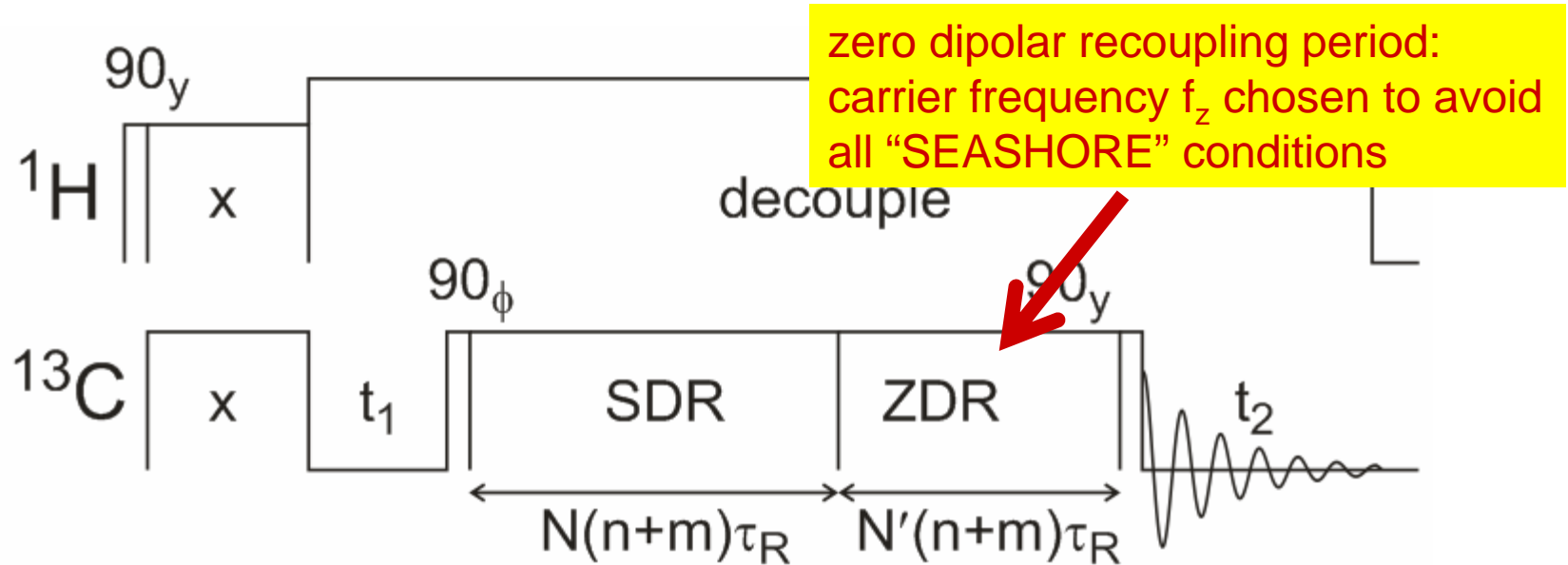
Ratio of oscillation periods = 1.61^3

Ratio of 50% decay times = 1.62^6



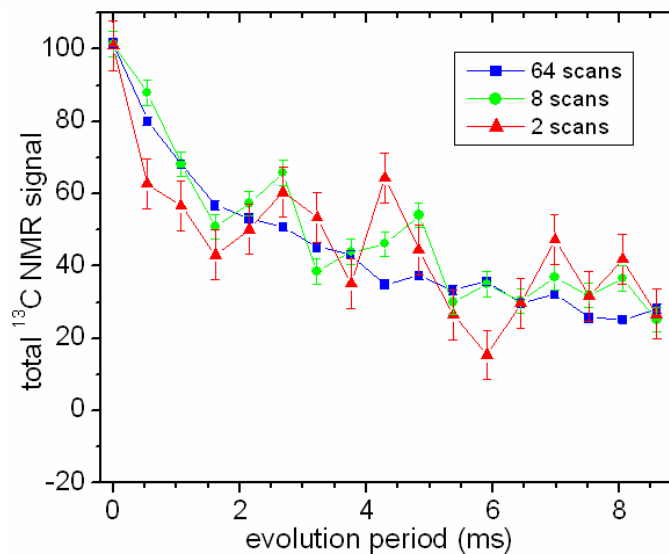
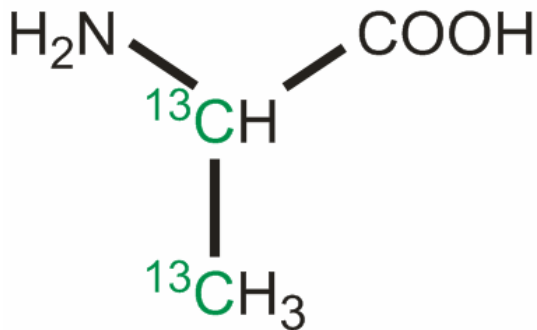
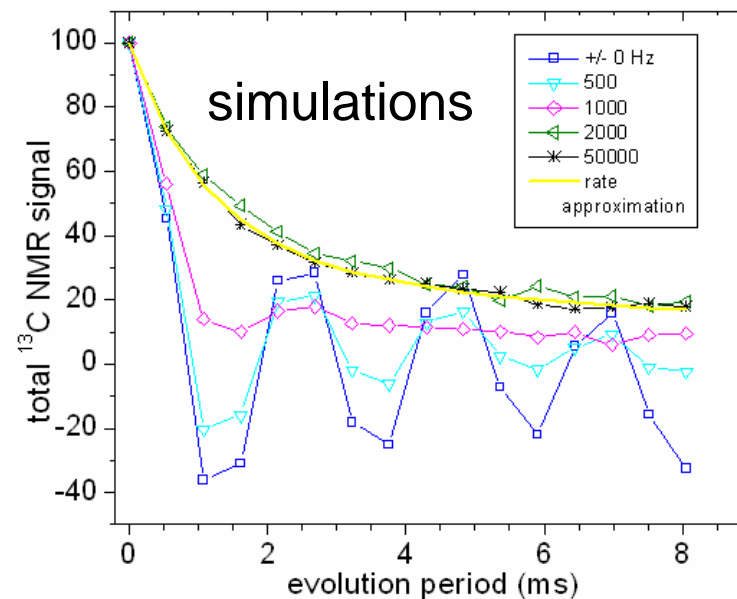
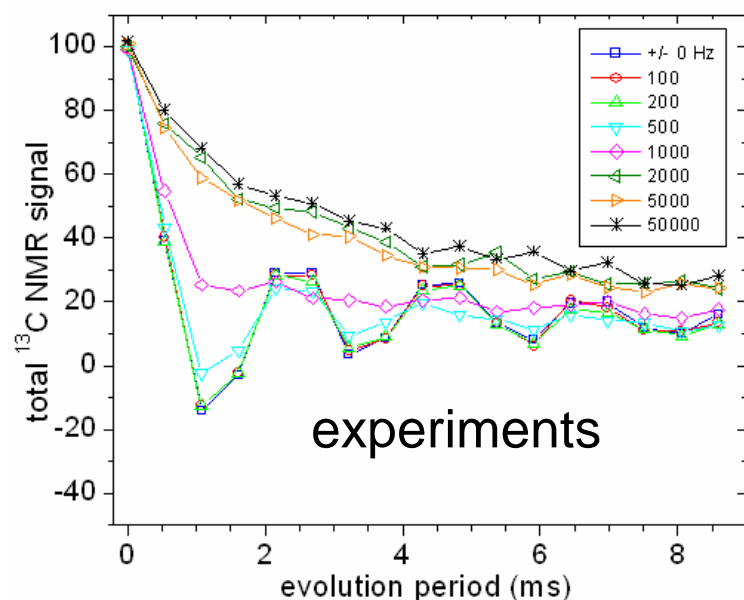
(POST-C7 recoupling, 7.45 kHz MAS, 9.4 T)

“Constant-time” stochastic dipolar recoupling



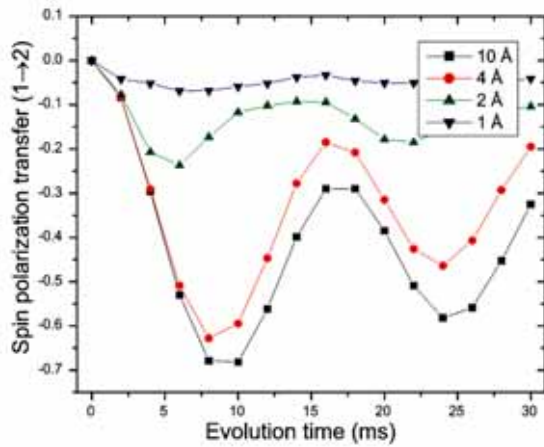
Experimental demonstrations of stochastic recoupling, two-spin systems

dependence on the range of carrier jumps between recoupling blocks

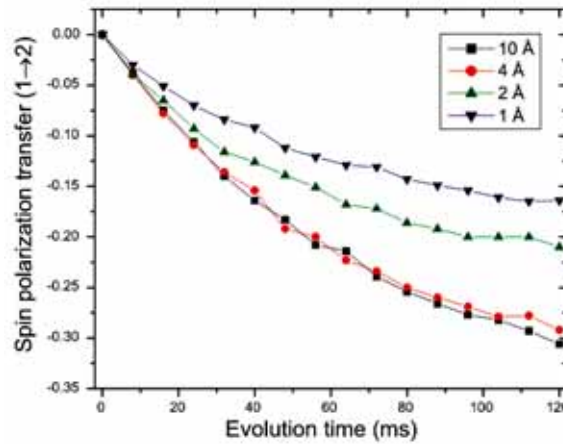


dependence on the number of scans per point

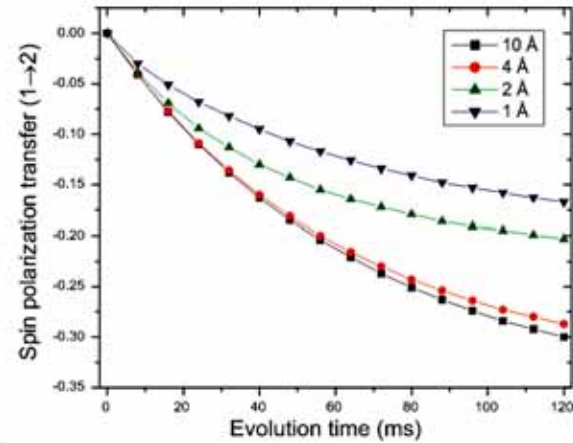
Simulations for three-spin systems



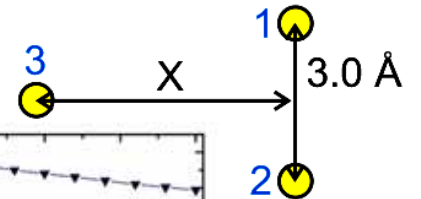
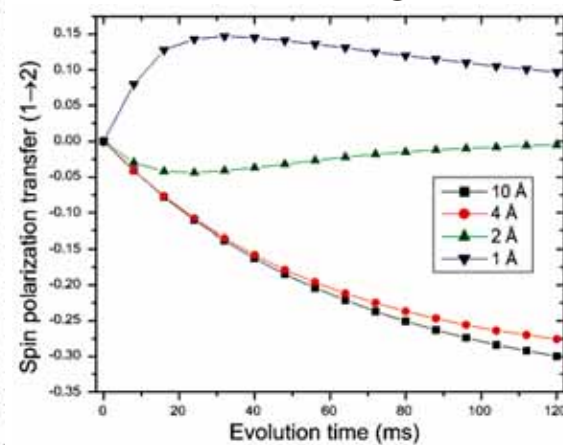
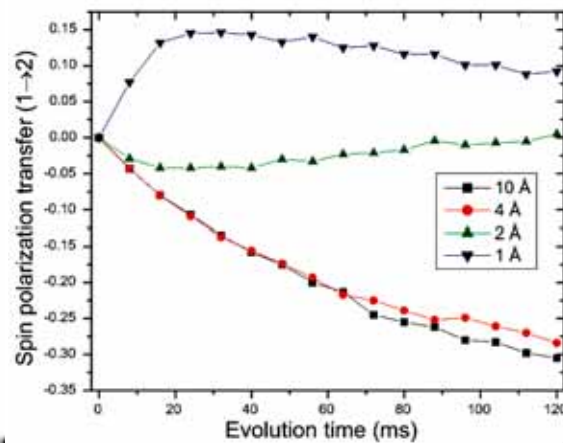
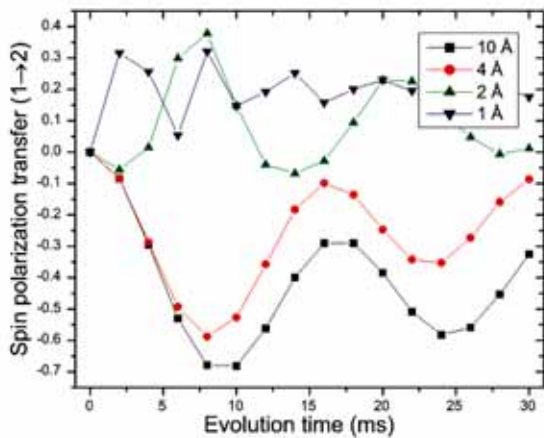
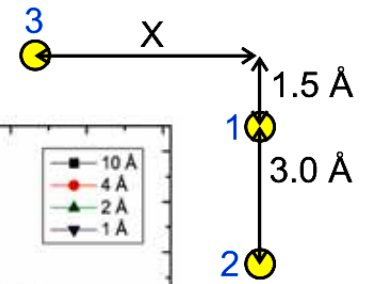
coherent



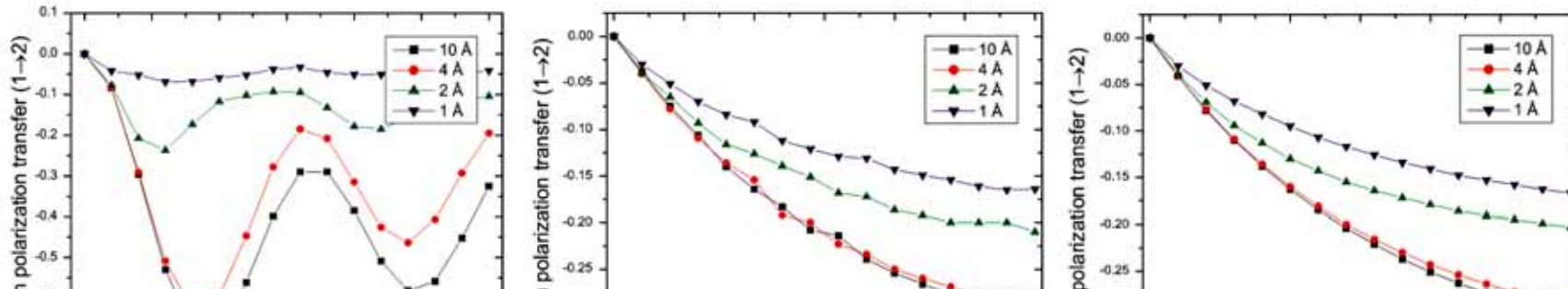
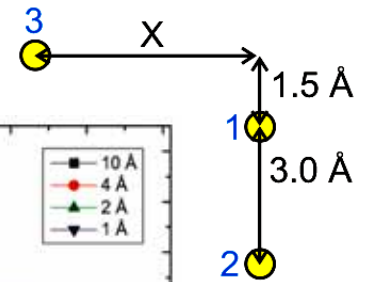
stochastic



rate approximation



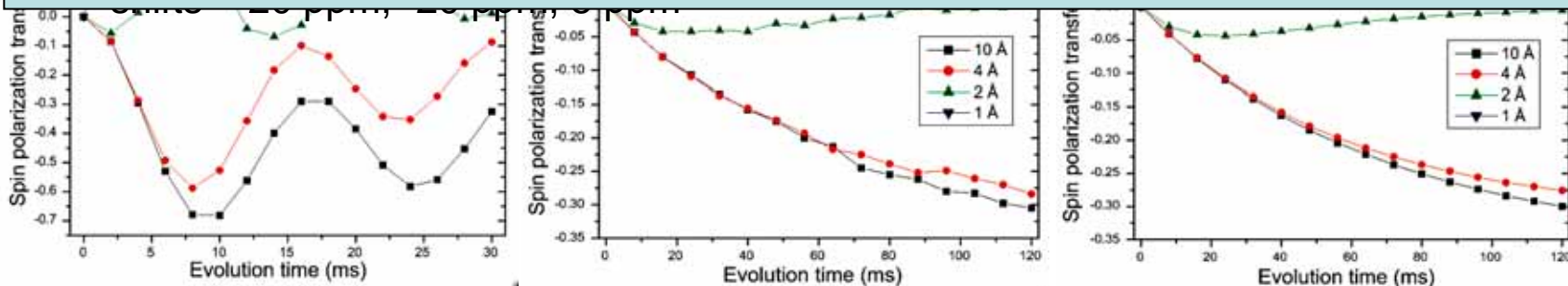
Simulations for three-spin systems



Rate approximation for spin polarization transfers after N recoupling blocks:

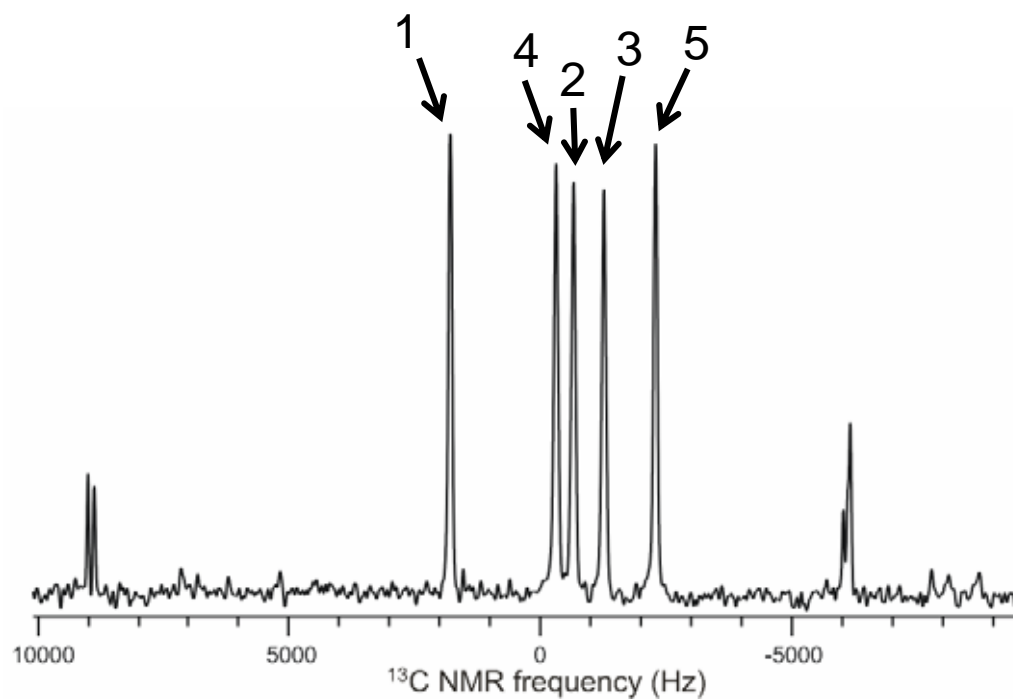
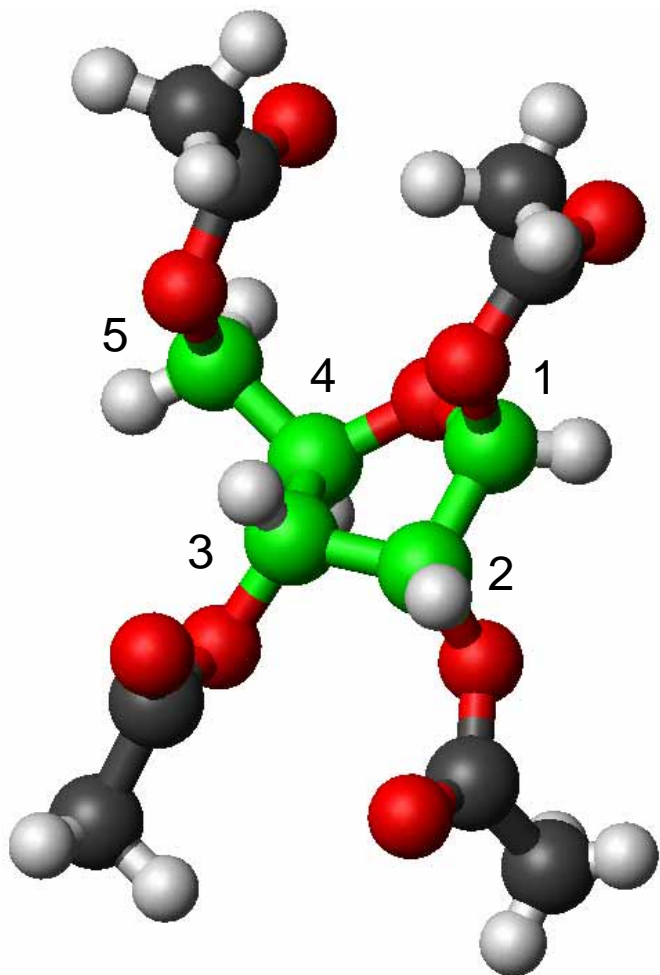
$\mathbf{p}(N) = \mathbf{W}^N \bullet \mathbf{p}(0)$ where $\mathbf{p}(N)$ is an n-dimensional polarization vector and \mathbf{W} is an n X n “rate matrix” with elements $W_{ij} = -\sin^2 \frac{1}{2} n d_{ij} \tau_R$

$$W_{jj} = 1 + \sum_{i \neq j} W_{ij}$$



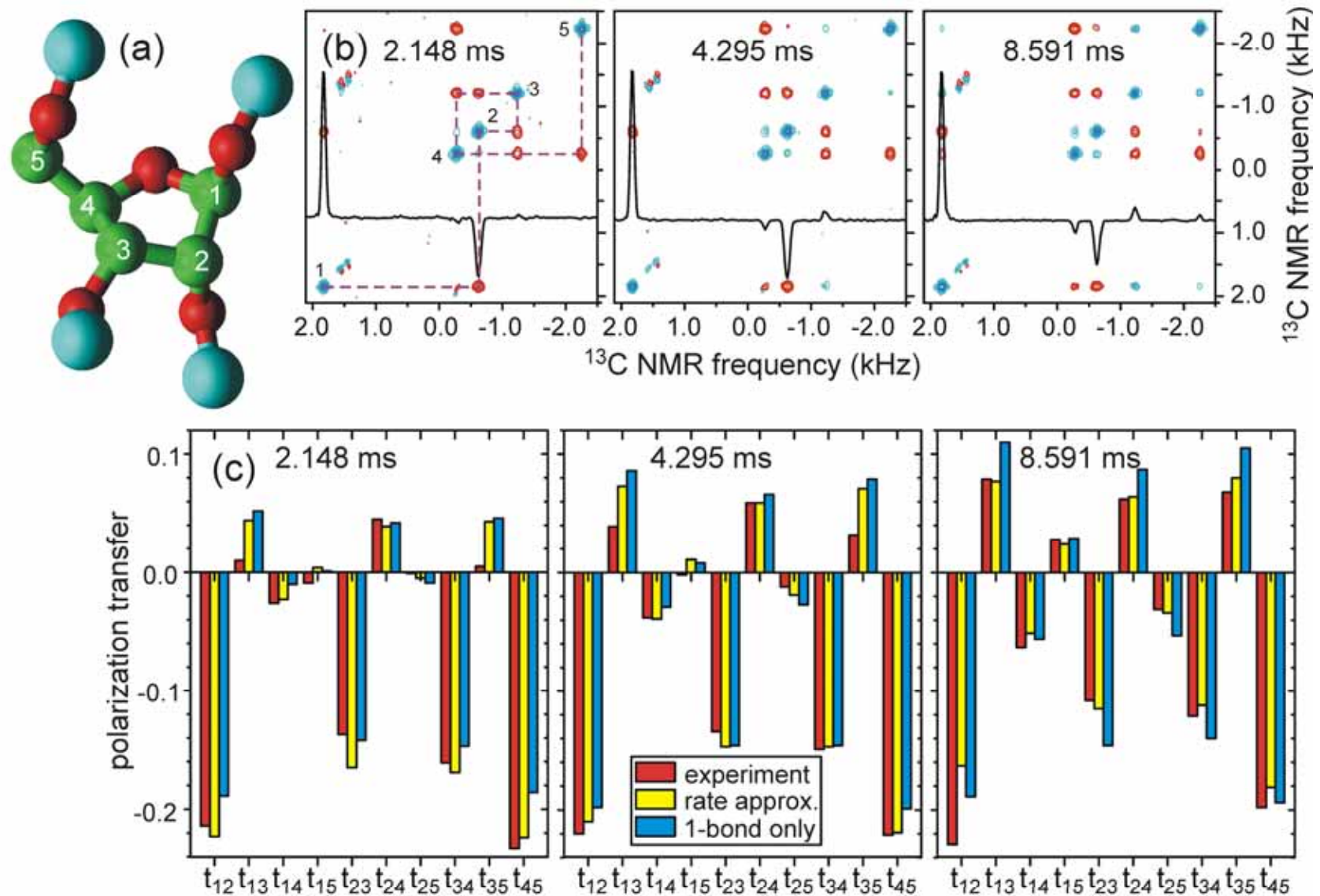
Stochastic recoupling, 5-spin system

β -D-ribofuranose tetraacetate (rfta)



(9% $^{13}\text{C}_5$ -rfta, diluted in unlabeled rfta)

Stochastic recoupling, 5-spin system



see *Phys. Rev. Lett.* **99**, 187601 (2007)

Analytical theory of SDR for two-spin systems

Attila Szabo

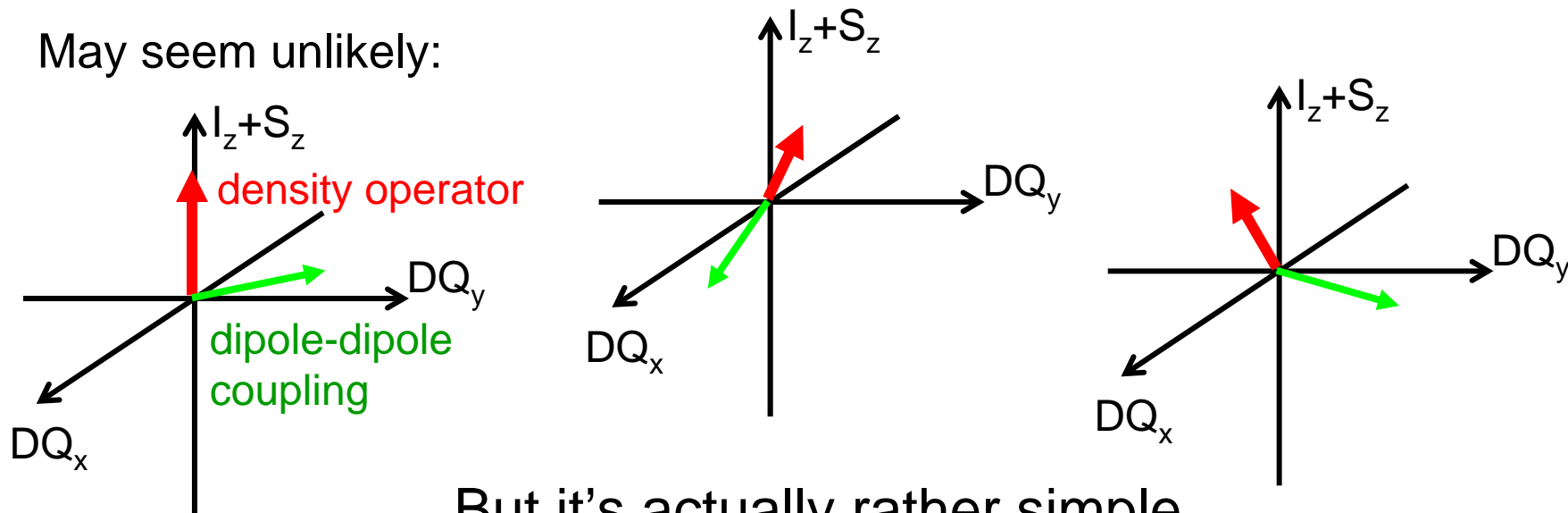


In the fully coherent limit ($f_{\max} = 0$), have oscillatory spin dynamics.

In the fully incoherent limit ($f_{\max} \tau_R \gg 1$), have exponential approach to equilibrium.

Is there an analytical expression that describes the SDR data for arbitrary f_{\max} ?

May seem unlikely:



But it's actually rather simple ...

During the SDR pulse sequence, the effective spin Hamiltonian alternates between

$$\tilde{H}_D^{(0)} = \frac{\gamma^2 \hbar}{R^3} (gI_{+1}I_{+2} + g^* I_{-1}I_{-2}) \quad \text{dipole-dipole coupling}$$

and

$$\tilde{H}_{CS}^{(0)}(k) = \frac{1}{2}(\delta_1 + \delta_2 + 2f_k)(I_{z1} + I_{z2}) + \frac{1}{2}(\delta_1 - \delta_2)(I_{z1} - I_{z2}) \quad \text{isotropic chemical shifts}$$

With $\delta_1 + \delta_2 \equiv 0$ at $f_k = 0$, the net evolution operator after N blocks can then be written as

$$U(N) = \exp[-iNm(\delta_1 - \delta_2)\tau_R J_\Delta] \exp(iJ_\Sigma \alpha) \quad \text{x rotation}$$

$$\times \left\{ \prod_{k=1}^N \left\{ \exp(-i2mf_k \tau_R J_\Sigma) \exp(-ind_{12} \tau_R J_x) \right\} \right\} \exp(-iJ_\Sigma \alpha)$$

random z rotation

$$J_\Sigma \equiv \frac{1}{2}(I_{z1} + I_{z2}) \quad J_\Delta \equiv \frac{1}{2}(I_{z1} - I_{z2})$$

where the “fictitious spin-1/2 operators” are defined by

$$J_x \equiv \frac{1}{2}(I_{+1}I_{+2} + I_{-1}I_{-2}) \quad J_y \equiv -\frac{i}{2}(I_{+1}I_{+2} - I_{-1}I_{-2})$$

and where

$$g = |g| e^{i\alpha}$$

$$d_{12} \equiv \frac{2\gamma^2 \hbar}{R^3} |g|$$

Assume that spins 1 and 2 are initially polarized along z:

$$\rho(0) = p_1(0)I_{z1} + p_2(0)I_{z2} = p_{\Delta}(0)J_{\Delta} + p_{\Sigma}(0)J_{\Sigma}$$

The density operator after N blocks must then have the form

$$\rho(N) = p_{\Delta}(0)J_{\Delta} + p_{\Sigma}(0)[u(N)J_x + v(N)J_y + w(N)J_{\Sigma}]$$

The quantity of interest, which determines the SDR NMR signals, is:

$$\begin{aligned} \langle w(N) \rangle &= \left\langle (0,0,1) \cdot \prod_{k=1}^N R_{\Sigma}(\theta_{\Sigma}(k)) R_x(\theta_x) \cdot \begin{pmatrix} 0 \\ 0 \\ 1 \end{pmatrix} \right\rangle \\ &= (0,0,1) \cdot \prod_{k=1}^N \langle R_{\Sigma}(\theta_{\Sigma}(k)) \rangle R_x(\theta_x) \cdot \begin{pmatrix} 0 \\ 0 \\ 1 \end{pmatrix} \end{aligned}$$

This can be calculated explicitly, because the random “ Σ ” rotations are all drawn from the same distribution.

Notes: --Does not assume that the two spins are spin-1/2 nuclei.
 --This is a “Liouville” description. Equivalent “Schrodinger” description seems intractable.

The rotation matrices are:

$$R_x(\theta_x) = \begin{pmatrix} 1 & 0 & 0 \\ 0 & \cos \theta_x & -\sin \theta_x \\ 0 & \sin \theta_x & \cos \theta_x \end{pmatrix}$$

$$\langle R_\Sigma(\theta_\Sigma) \rangle = \begin{pmatrix} \langle \cos \theta_\Sigma \rangle & -\langle \sin \theta_\Sigma \rangle & 0 \\ \langle \sin \theta_\Sigma \rangle & \langle \cos \theta_\Sigma \rangle & 0 \\ 0 & 0 & 1 \end{pmatrix} = \begin{pmatrix} \frac{1}{\theta_{\max}} \sin \theta_{\max} & 0 & 0 \\ 0 & \frac{1}{\theta_{\max}} \sin \theta_{\max} & 0 \\ 0 & 0 & 1 \end{pmatrix}$$

which implies that

$$\langle w(N) \rangle = (0,0,1) \cdot \begin{pmatrix} \frac{1}{\theta_{\max}} \sin \theta_{\max} & 0 & 0 \\ 0 & \frac{1}{\theta_{\max}} \sin \theta_{\max} \cos \theta_x & -\frac{1}{\theta_{\max}} \sin \theta_{\max} \sin \theta_x \\ 0 & \sin \theta_x & \cos \theta_x \end{pmatrix}^N \cdot \begin{pmatrix} 0 \\ 0 \\ 1 \end{pmatrix}$$

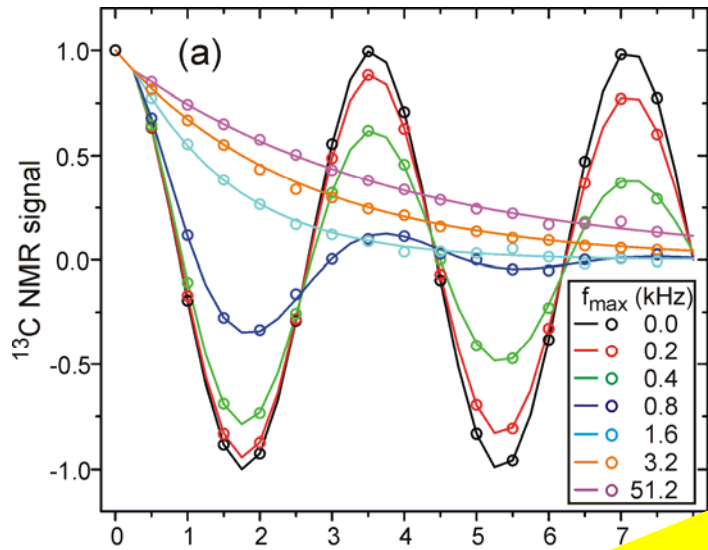
By diagonalizing the non-Hermitian 2 X 2 matrix (with complex eigenvalues and non-orthogonal eigenvectors):

$$\langle w(N) \rangle = \frac{\varepsilon_+^N (\cos \theta_x - \varepsilon_-) - \varepsilon_-^N (\cos \theta_x - \varepsilon_+)}{\varepsilon_+ - \varepsilon_-}$$

final result

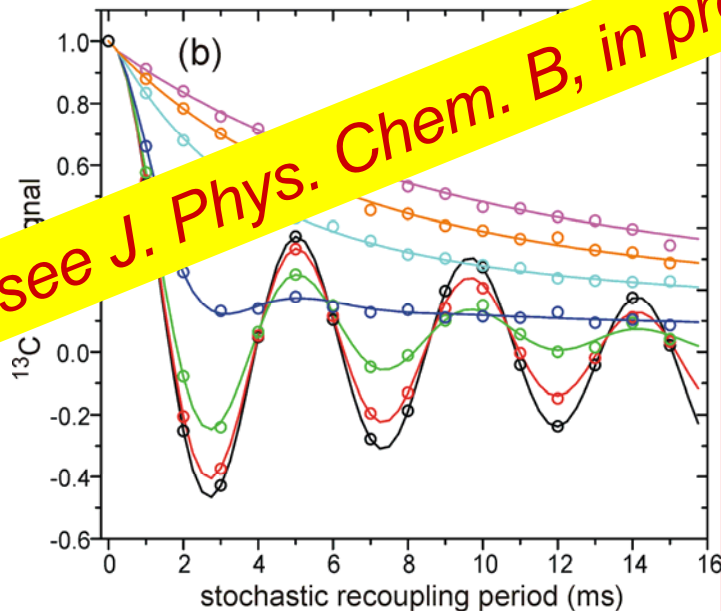
$$\varepsilon_{\pm} = \frac{1}{2} \left(1 + \frac{\sin \theta_{\max}}{\theta_{\max}} \right) \cos \theta_x \pm \frac{1}{2} \sqrt{\left(1 + \frac{\sin \theta_{\max}}{\theta_{\max}} \right)^2 \cos^2 \theta_x - 4 \frac{\sin \theta_{\max}}{\theta_{\max}}}$$

Comparison of exact (lines) and numerical (circles) calculations

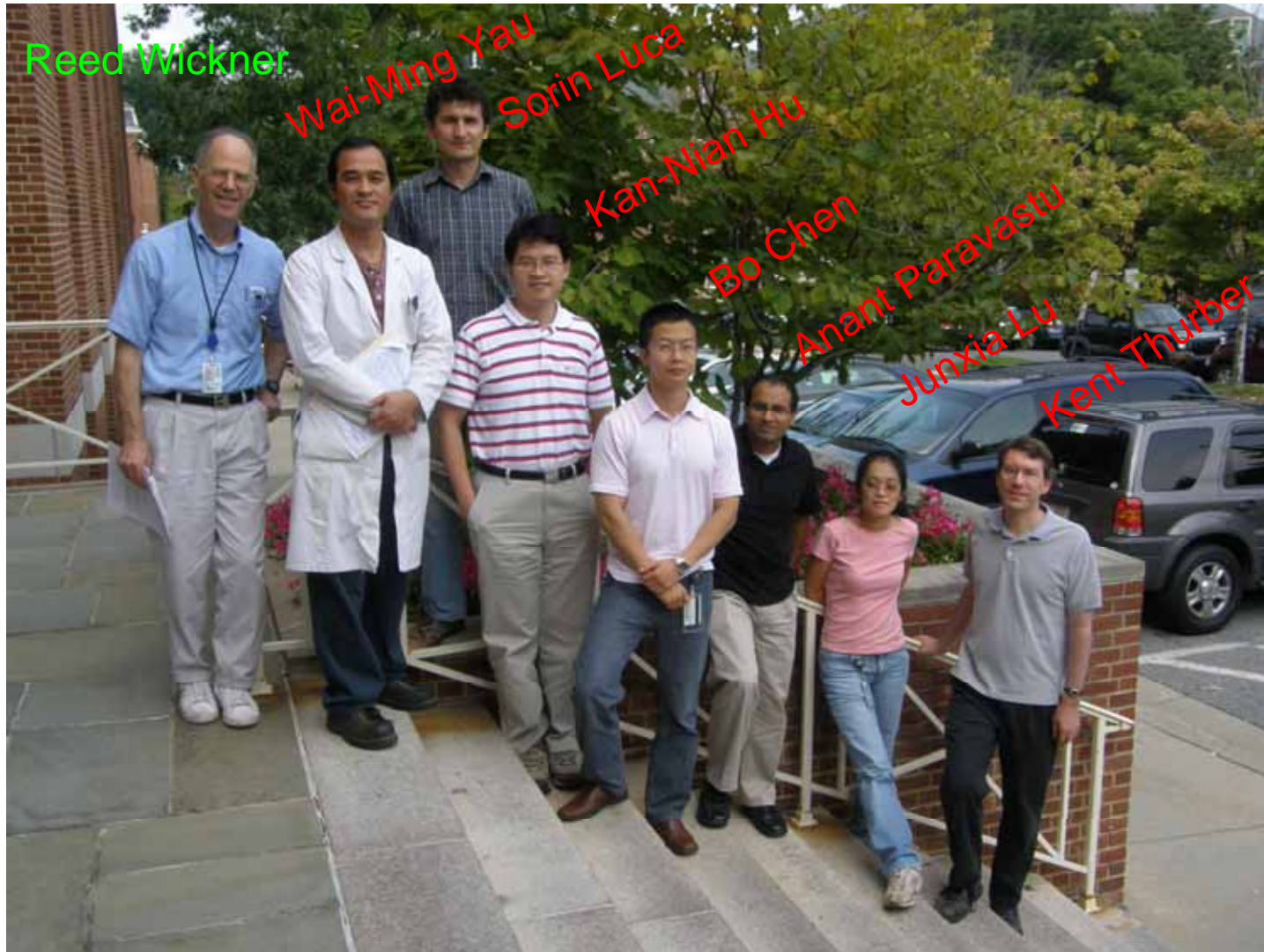


^{13}C spin pairs, 3.0 Å distance, $g = \frac{1}{2}$,
 $\tau_R = 125 \mu\text{s}$, $n = 2$, and $m = 1$.

see J. Phys. Chem. B, in press (Attila Szabo festschrift)



^{13}C spin pairs, 2.0 Å internuclear distance, POST-C7 sequence, $\tau_R = 125 \mu\text{s}$, $n = 2$, and $m = 1$. Exact calculations use orientation-dependent g values extracted from the numerically determined propagator for DQ periods.



Supported by the Intramural Research Program of the National Institute of Diabetes and Digestive and Kidney Diseases (NIDDK) and by the NIH Intramural AIDS Targeted Antiviral Program (IATAP).